

# Leprosy drug clofazimine activates peroxisome proliferator-activated receptor- $\gamma$ and synergizes with imatinib to inhibit chronic myeloid leukemia cells



Harish Kumar,<sup>1</sup> Sourav Chattopadhyay,<sup>1,2</sup> Nabanita Das,<sup>1</sup> Sonal Shree,<sup>3</sup> Dinesh Patel,<sup>4</sup> Jogeswar Mohapatra,<sup>4</sup> Anagha Gurjar,<sup>1,2</sup> Sapana Kushwaha,<sup>1</sup> Abhishek Kumar Singh,<sup>1</sup> Shikha Dubey,<sup>3</sup> Kiran Lata,<sup>3</sup> Rajesh Kushwaha,<sup>5</sup> Riyazuddin Mohammed,<sup>6</sup> Krishnarup Ghosh Dastidar,<sup>4</sup> Namrata Yadav,<sup>4</sup> Achchhe Lal Vishwakarma,<sup>7</sup> Jiaur Rahaman Gayen,<sup>6,2</sup> Sanghamitra Bandyopadhyay,<sup>5</sup> Abhijit Chatterjee,<sup>4</sup> Mukul Rameshchandra Jain,<sup>4</sup> Anil Kumar Tripathi,<sup>8</sup> Arun Kumar Trivedi,<sup>1,2</sup> Naibedy Chattopadhyay,<sup>9,2</sup> Ravishankar Ramachandran<sup>2,3</sup> and Sabyasachi Sanyal<sup>1,2</sup>

<sup>1</sup>Division of Biochemistry, CSIR-Central Drug Research Institute, Lucknow; <sup>2</sup>AcSIR, CSIR-Central Drug Research Institute Campus, Lucknow; <sup>3</sup>Division of Molecular and Structural Biology, CSIR-Central Drug Research Institute, Lucknow; <sup>4</sup>Zydus Research Center, Moraiya, Ahmedabad, Gujarat; <sup>5</sup>Developmental Toxicology Laboratory, Systems Toxicology and Health Risk Assessment Group, CSIR-Indian Institute of Toxicology Research, Lucknow; <sup>6</sup>Pharmacokinetics and Metabolism Division, CSIR-Central Drug Research Institute, Lucknow; <sup>7</sup>Sophisticated Analytical Instrument Facility, CSIR-Central Drug Research Institute, Lucknow; <sup>8</sup>Department of Clinical Hematology and Medical Oncology, King George's Medical University, Lucknow, Uttar Pradesh and <sup>9</sup>Division of Endocrinology, CSIR-Central Drug Research Institute, Lucknow, India

## ABSTRACT

Leukemia stem cells contribute to drug-resistance and relapse in chronic myeloid leukemia (CML) and BCR-ABL1 inhibitor monotherapy fails to eliminate these cells, thereby necessitating alternate therapeutic strategies for patients CML. The peroxisome proliferator-activated receptor- $\gamma$  (PPAR $\gamma$ ) agonist pioglitazone downregulates signal transducer and activator of transcription 5 (STAT5) and in combination with imatinib induces complete molecular response in imatinib-refractory patients by eroding leukemia stem cells. Thiazolidinediones such as pioglitazone are, however, associated with severe side effects. To identify alternate therapeutic strategies for CML we screened Food and Drug Administration-approved drugs in K562 cells and identified the leprosy drug clofazimine as an inhibitor of viability of these cells. Here we show that clofazimine induced apoptosis of blood mononuclear cells derived from patients with CML, with a particularly robust effect in imatinib-resistant cells. Clofazimine also induced apoptosis of CD34<sup>+</sup>38<sup>+</sup> progenitors and quiescent CD34<sup>+</sup> cells from CML patients but not of hematopoietic progenitor cells from healthy donors. Mechanistic evaluation revealed that clofazimine, via physical interaction with PPAR $\gamma$ , induced nuclear factor  $\kappa$ B-p65 proteasomal degradation, which led to sequential myeloblastoma oncoprotein and peroxiredoxin 1 downregulation and concomitant induction of reactive oxygen species-mediated apoptosis. Clofazimine also suppressed STAT5 expression and consequently downregulated stem cell maintenance factors hypoxia-inducible factor-1 $\alpha$  and -2 $\alpha$  and Cbp/P300 interacting transactivator with Glu/Asp-rich carboxy-terminal domain 2 (CITED2). Combining imatinib with clofazimine caused a far superior synergy than that with pioglitazone, with clofazimine reducing the half maximal inhibitory concentration (IC<sub>50</sub>) of imatinib by >4 logs and remarkably eroding quiescent CD34<sup>+</sup> cells. In a K562 xenograft study clofazimine and imatinib co-treatment showed more robust efficacy than the individual treatments. We propose clinical evaluation of clofazimine in imatinib-refractory CML.

Haematologica 2020  
Volume 105(4):971-986

## Correspondence:

SABYASACHI SANYAL  
sanyal@cdri.res.in

Received: April 11, 2019

Accepted: July 12, 2019.

Pre-published: August 1, 2019.

doi:10.3324/haematol.2018.194910

Check the online version for the most updated information on this article, online supplements, and information on authorship & disclosures: [www.haematologica.org/content/105/4/971](http://www.haematologica.org/content/105/4/971)

©2020 Ferrata Storti Foundation

Material published in Haematologica is covered by copyright. All rights are reserved to the Ferrata Storti Foundation. Use of published material is allowed under the following terms and conditions:

<https://creativecommons.org/licenses/by-nc/4.0/legalcode>.

Copies of published material are allowed for personal or internal use. Sharing published material for non-commercial purposes is subject to the following conditions:

<https://creativecommons.org/licenses/by-nc/4.0/legalcode>, sect. 3. Reproducing and sharing published material for commercial purposes is not allowed without permission in writing from the publisher.



## Introduction

The therapy of chronic myeloid leukemia (CML) has seen tremendous advances following the discovery of imatinib and other BCR-ABL1 tyrosine kinase inhibitors. However, complete molecular response, defined as undetectable *BCR-ABL1* transcripts, is not achieved in the majority of patients.<sup>1</sup> Resistance to tyrosine kinase inhibitors may occur due to *BCR-ABL1* mutations; however, in approximately 50% of the cases BCR-ABL1-independent mechanisms, including tyrosine kinase inhibitor-refractory leukemia stem cells (LSC), contribute to resistance and recurrence.<sup>1</sup> Therefore therapeutic approaches capable of overcoming resistance to tyrosine kinase inhibitors are needed. Peroxisome proliferator-activated receptor- $\gamma$  (PPAR $\gamma$ ) agonists, pioglitazone in particular, were reported to erode quiescent LSC by targeting signal transducer and activator of transcription 5 (STAT5) expression.<sup>1,2</sup> Unfortunately, pioglitazone increases the risk of bladder cancer.<sup>3</sup> Although rosiglitazone has not been found to increase the incidence of bladder cancer, it is associated with severe cardiovascular risks.<sup>4</sup>

To identify new therapeutic strategies we screened 800 Food and Drug Administration-approved drugs for their anti-CML efficacy in the K562 cell line and identified clofazimine as a potent inhibitor of viability. Clofazimine, a riminophenazine leprosy drug, is also effective against multidrug-resistant tuberculosis<sup>5</sup> and imparts its anti-bacterial actions by generating reactive oxygen species (ROS), particularly superoxides and hydrogen peroxide (H<sub>2</sub>O<sub>2</sub>).<sup>6</sup> Clofazimine also displays anti-inflammatory properties that are important for its suppression of leprosy-associated immune reactions.<sup>6</sup> Additionally, clofazimine was shown to be effective against various autoimmune diseases, including discoid lupus erythematosus, Crohn disease, ulcerative colitis, psoriasis, Meischer granuloma and graft-versus-host disease.<sup>7</sup> Clofazimine is reported to exert its immunomodulatory activities by blocking KV1.3 voltage-gated potassium channels<sup>7</sup> and thereby inhibiting chronic lymphocytic leukemia cells.<sup>8,9</sup>

Here we report the anti-CML efficacy of clofazimine in cells lacking KV1.3,<sup>8,10</sup> and show that clofazimine exerted its effects by binding to PPAR $\gamma$ . Clofazimine not only suppressed STAT5 expression by modulating PPAR $\gamma$  transcriptional activity but also regulated a novel signaling cascade by increasing PPAR $\gamma$ -mediated p65 nuclear factor kappa B (NF $\kappa$ B) degradation, which caused transcriptional downregulation of cellular myeloblastoma oncoprotein (MYB), leading to suppression of peroxiredoxin 1 (PRDX1) expression and consequent induction of ROS-mediated apoptosis and differentiation.

## Methods

### Cell lines and human primary cells

K562 (CCL-243), HL-60 (CCL-240), U937 (CRL-1593.2), and HEK-293 (CRL-1573) cells were from the American Type Culture Collection (ATCC; Manassas, VA, USA) and were maintained as per ATCC instructions. Peripheral blood samples were obtained from BCR-ABL1<sup>+</sup> CML patients (newly diagnosed, imatinib-resistant and imatinib responders), and healthy donors from King George's Medical University (Clinical Hematology and Medical Oncology Division, Lucknow, India) following ethical approval (approval n. 1638/R. Cell-12) as per institutional ethical guidelines

after written consent (patients' details in *Online Supplementary Table S1*). Peripheral blood mononuclear cells were isolated on a Percoll (Sigma) density gradient by centrifugation. All analyses of peripheral blood mononuclear cells were conducted on gated mononuclear cells excluding lymphocytes.

### Other methods

Chemicals, antibodies, plasmid information and experimental procedures are detailed in the *Online Supplementary Methods*.

### Statistical analysis

Data are expressed as the mean  $\pm$  standard error of mean of three independent experiments, unless otherwise indicated. Statistical analyses were performed using GraphPad Prism 5.0. An unpaired two-tailed Student *t*-test or Mann-Whitney U test was used to compare two groups. Equality of variances was assessed by the F-test. Statistical analyses involving more than two groups were performed by one- or two-way analysis of variance followed by the Bonferroni post-test, or Kruskal-Wallis test followed by the Dunn test. For intra-group variances, we used the Levene median test (equal sample size; using XLSTAT) or Bartlett test (unequal sample size). *P*<0.05 was accepted as statistically significant.

## Results

### Clofazimine induces apoptosis and differentiation in chronic myeloid leukemia cells

In a screening in K562 cells, we identified clofazimine as a potent inhibitor of viability. Clofazimine has been reported to induce cytotoxicity by targeting KV1.3.<sup>7-9</sup> Intriguingly, although K562 does not express KV1.3,<sup>8,10</sup> (*Online Supplementary Figure S1A*), clofazimine reduced the viability of these cells with a pharmacologically relevant half maximal inhibitory concentration (IC<sub>50</sub>) of 5.85  $\mu$ M (Figure 1A). The human plasma C<sub>max</sub> of clofazimine is 0.4-4 mg/L, equivalent to 0.84-8.4  $\mu$ M.<sup>6,11-13</sup> The loss of viability was due to apoptosis, as demonstrated by annexin V staining (Figure 1B, *Online Supplementary Figure S1B*), poly (ADP-ribose) polymerase (PARP) cleavage (Figure 1C) and terminal deoxynucleotidyl transferase dUTP nick end labeling (TUNEL) (*Online Supplementary Figure S1C*). Clofazimine induced cytochrome C release and activated caspase -3 and -9 but not -8 (Figure 1D), suggesting mitochondria-mediated apoptosis, which was consistent with decreased B-cell lymphoma 2 (BCL-2) and increased BAX expression (Figure 1D). Clofazimine also induced apoptosis in peripheral blood mononuclear cells from patients with chronic phase CML (CP-CML cells; one newly diagnosed patient was in accelerated phase, one imatinib-responder was in blast crisis) with an efficacy similar to that of cells from patients with newly diagnosed CML and imatinib-responders but higher than that of imatinib and dasatinib in imatinib-resistant cells, while it did not affect healthy donor cells (Figure 1E, *Online Supplementary Figure S1D*). Among the 21 imatinib-resistant patients (Figure 1E), seven harbored the following *BCR-ABL1* mutations; M244V (n=1), Y253H (n=2), M351T (n=3) and F359V (n=1); clofazimine showed efficacy in all cases (Figure 1F; upper panel). A separate analysis of apoptosis in imatinib-resistant patients without *BCR-ABL1* mutations (from Figure 1E) also showed significant clofazimine-induced apoptosis (n=6: vehicle, imatinib, clofazimine; n=5; dasatinib. Figure 1F; lower panel), indicating that clofazimine-

induced apoptosis in imatinib-resistant cells is independent of *BCR-ABL1* mutations.

We next assessed whether clofazimine inhibited LSC. Increased aldehyde dehydrogenase activity is a hallmark of cancer stem cells<sup>14</sup> and clofazimine reduced it in imatinib-resistant CP-CML cells at par with the positive control salinomycin (Figure 1G, *Online Supplementary Figure S2A*). Clofazimine also reduced colony formation in CML CD34<sup>+</sup> cells (Figure 1H, *Online Supplementary Figure S2C*). To further confirm its anti-LSC efficacy we treated purified CML CD34<sup>+</sup> cells with clofazimine and analyzed them by CD34 or annexin V staining. Clofazimine reduced the CD34<sup>+</sup> population and induced apoptosis in these cells (Figure 1I, *Online Supplementary Figure S2B*). Treating CML CD34<sup>+</sup> cells with clofazimine and analyzing them by CD34, CD38 and annexin V co-staining revealed that clofazimine induced apoptosis in both committed CD34<sup>+</sup>38<sup>+</sup> and primitive CD34<sup>+</sup>38<sup>-</sup> progenitor cells (Figure 1J). Clofazimine however, caused <5% loss in viability and no apoptosis in hematopoietic progenitor cells from healthy donors (Figure 1K, L, *Online Supplementary Figure S2D*) indicating that it specifically targets LSC. Clofazimine's effects in CML CD34<sup>+</sup> cells were not routed through KV1.3 as KV1.3 transcript was undetectable in CD34<sup>+</sup>-enriched CP-CML cells (n=7; *Online Supplementary Figure S3*).

We next investigated whether clofazimine induced differentiation at sub-lethal concentrations. In K562 cells that

predominantly undergo erythroid or megakaryocytic differentiation upon various stimuli, clofazimine induced a megakaryocyte-like phenotype characterized by increased cellular size, nuclear to cytoplasmic ratio, vacuolation, and lobulated nuclei (*Online Supplementary Figure S4A*). Consistently, clofazimine increased megakaryocytic surface markers CD61 and CD41 in K562 (*Online Supplementary Figure S4B-D*) and CML (one newly diagnosed patient was in accelerated phase, one imatinib-resistant patient was in blast crisis) cells (Figure 1M, *Online Supplementary Figure S4E-F*). Clofazimine treatment in CML CD34<sup>+</sup> cells followed by May-Grünwald-Giemsa staining revealed increased monocyte-like morphology (Figure 1N, *Online Supplementary Figure S4G*). Concurrently, expression of the monocyte/macrophage differentiation marker CD11b was increased in clofazimine-treated CD34<sup>+</sup> cells (Figure 1O, *Online Supplementary Figure S4H*). Furthermore, clofazimine also induced CD61 in CD34<sup>+</sup> cells (Figure 1P, *Online Supplementary Figure S4H*).

### Apoptosis- and differentiation-inducing effects of clofazimine are associated with enhanced reactive oxygen species and decreased PRDX1 expression

We next asked how clofazimine exerts its action and decided to address its differentiation-inducing activity first. Megakaryocytic differentiation in K562 cells is typically associated with prolonged extracellular signal-regu-

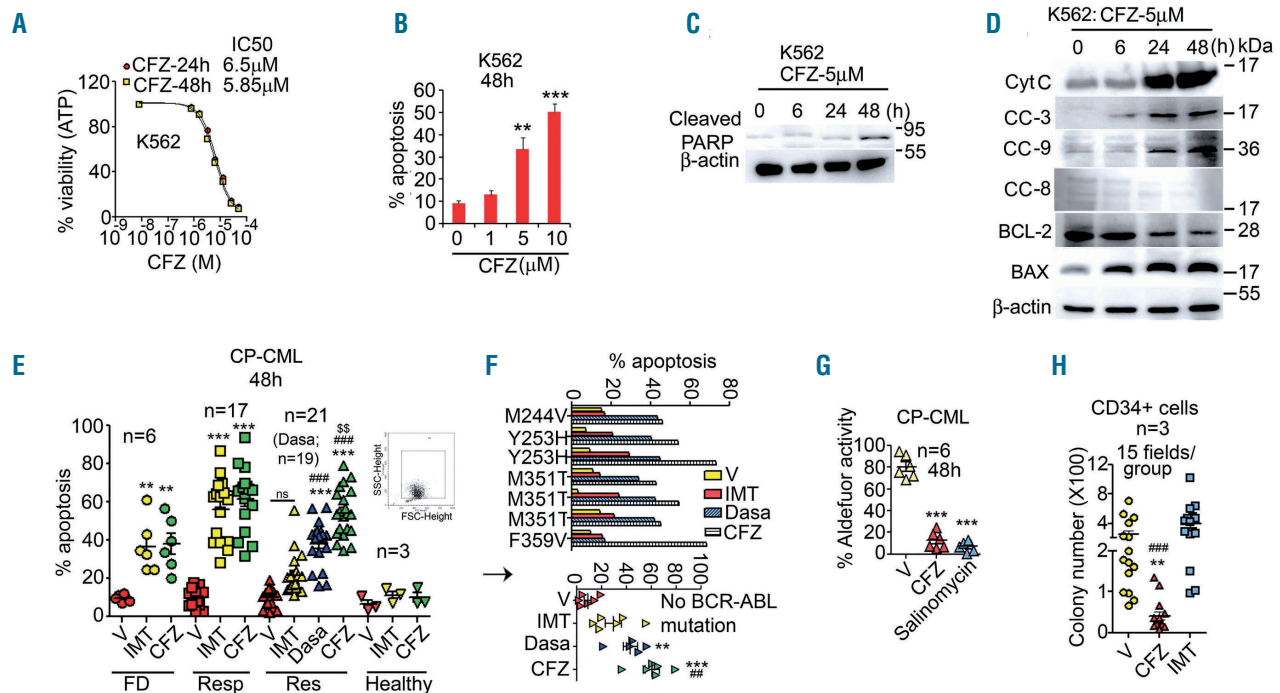


**Figure 1. Clofazimine induces apoptosis and differentiation in K562 and chronic phase chronic myeloid leukemia cells and reduces leukemia stem cell load.** (A, B) Clofazimine (CFZ) reduces K562 cell viability and induces apoptosis. (A) CFZ dose response, as determined by a CellTiter-Glo assay. (B) Apoptosis (n=3; representative dot plot in *Online Supplementary Figure S1B*). (C) Poly (ADP-ribose) polymerase cleavage in K562 cells. (D) CFZ induces cytochrome C release, caspase cleavage, BAX expression and suppresses BCL-2 in K562 cells. (E, F) CFZ (all drugs 5  $\mu$ M) induces apoptosis in chronic phase chronic myeloid leukemia (CP-CML) cells (annexin/propidium iodide (PI) staining; dot plots in *Online Supplementary Figure S1D*). (F) Percentage apoptosis in cells from imatinib-resistant patients in Figure 1E, harboring the indicated *BCR-ABL1* mutations (upper panel) and CP-CML cells in which no *BCR-ABL1* mutations were detected (lower panel). (G) CFZ (or salinomycin; both at a concentration of 5  $\mu$ M) reduced aldehyde dehydrogenase activity, determined by percentage aldehyde activity in CP-CML cells (dot plots in *Online Supplementary Figure S2A*). (H) CFZ reduces the number of colony-forming cells in soft agar (images in *Online Supplementary Figure S2C*; imatinib 1  $\mu$ M, CFZ 2.5  $\mu$ M). (continued on next page)

lated kinase (ERK) activation.<sup>15,16</sup> Interestingly, mitogen-activated protein kinase (MAPK) kinase inhibitor U0126 failed to inhibit clofazimine but not phorbol myristate acetate (PMA)-induced CD41 expression (Figure 2A, *Online Supplementary Figure S5A*). Consistently, PMA but not clofazimine induced ERK phosphorylation in K562 cells (Figure 2B). Apart from ERK, ROS induces megakaryocytic differentiation<sup>17-19</sup> and determination of cellular ROS revealed that clofazimine significantly enhanced ROS production from 12 h onwards (Figure 2C, *Online Supplementary Figure S5B*). Clofazimine also enhanced mitochondrial superoxide (Figure 2D, E) and H<sub>2</sub>O<sub>2</sub> (Figure 2F) and caused mitochondrial membrane depolarization (Figure 2G, *Online Supplementary Figure S5C*). Co-treatment with ROS scavengers and inhibitors revealed that  $\alpha$ -

tocopherol, which interacts with superoxides<sup>20</sup> and also blocks H<sub>2</sub>O<sub>2</sub> and peroxynitrite-mediated toxicity,<sup>21-23</sup> completely abrogated clofazimine-induced cell death while the ROS scavenger N-acetyl-L-cysteine and H<sub>2</sub>O<sub>2</sub> decomposer catalase had lesser but significant effects, and the mitochondrial complex inhibitors rotenone and antimycin and the NADPH oxidase inhibitor diphenyleneiodonium were ineffective (Figure 2H).  $\alpha$ -tocopherol also inhibited clofazimine-induced CD41 and CD61 expression (Figure 2I, *Online Supplementary Figure S5D-F*). These results indicate that clofazimine induced ROS-dependent cell death and differentiation.

Cancer cells, including cancer stem cells, display high levels of ROS coupled with increased antioxidants that help them detoxify ROS.<sup>24-27</sup> We thus investigated whether

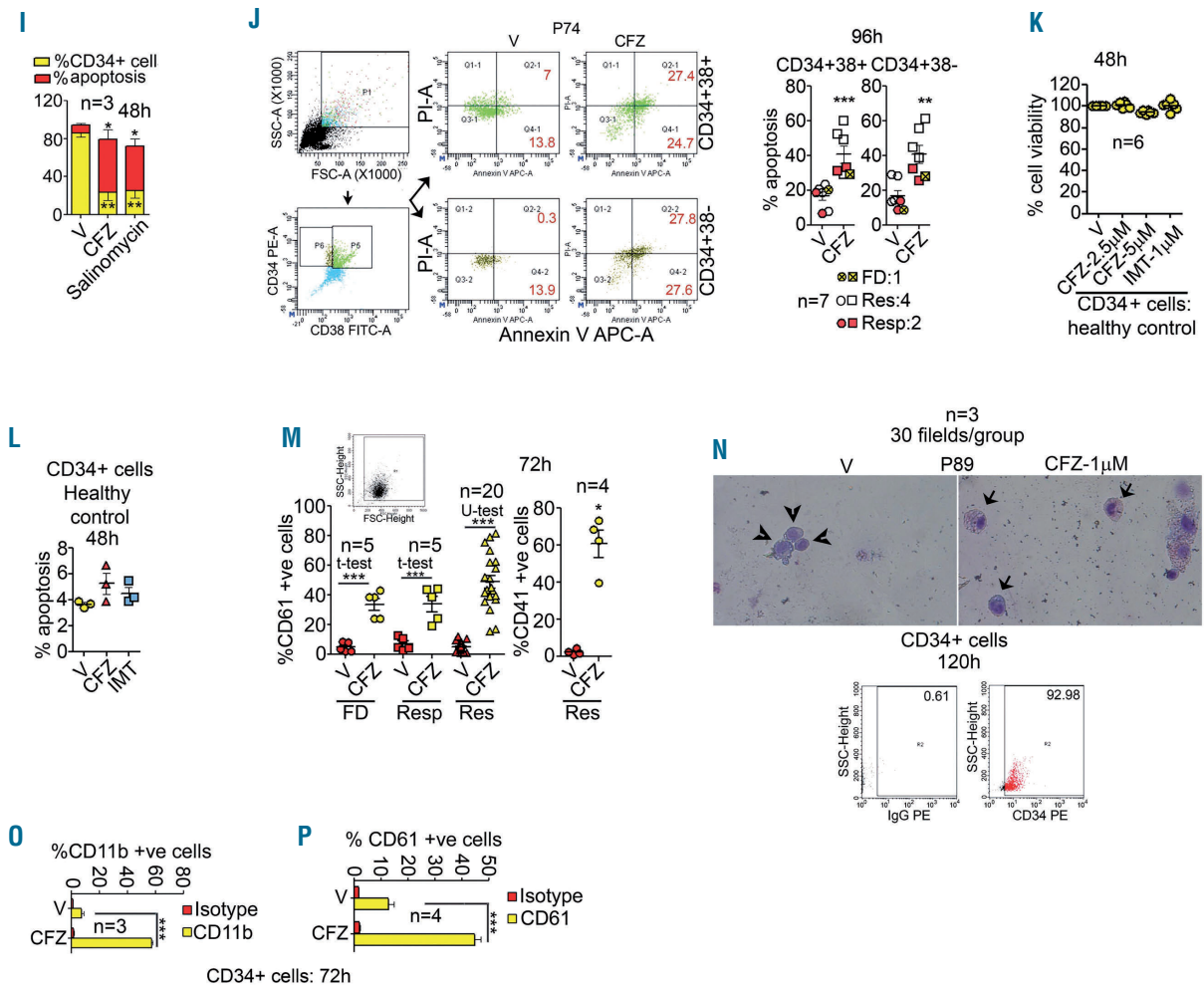


**Figure 1.** (continued from previous page) (I, J) CFZ induces apoptosis in CP-CML CD34<sup>+</sup> cells. (I) CD34<sup>+</sup> cells from imatinib-resistant patients were isolated using a CD34 microbead kit (Miltenyi Biotech) and were treated with 5  $\mu$ M CFZ or salinomycin for 48 h. Cells were then divided into two groups. One group was assessed by immunostaining for CD34 and the other group was stained with annexin V/PI and the cells were then analyzed by flow cytometry (dot plots in *Online Supplementary Figure S2B*). (J) The CD34<sup>+</sup> population from imatinib-resistant CP-CML cells was treated with CFZ (2.5  $\mu$ M) for 96 h, stained with anti-CD34 and anti-CD38 antibodies and assessed for apoptosis. (K, L) CFZ does not affect viability of hematopoietic progenitors from healthy controls. (K) Cell viability, determined by a CellTiter-Glo assay. (L) Apoptosis by annexin V staining (dot plots in *Online Supplementary Figure S2D*). (M) CFZ (1  $\mu$ M) induces CD61 and CD41 in CP-CML cells (dot plots in *Online Supplementary Figure S4E, F*). (N) CFZ induces monocyte-like morphology in CD34<sup>+</sup> cells (cropped images shown; corresponding original images in *Online Supplementary Figure S4G*). (O, P) CFZ (1  $\mu$ M) induces CD11b (O) and CD61 (P) in CD34<sup>+</sup> CP-CML cells (histograms in *Online Supplementary Figure S4H*). Graphs illustrate the mean  $\pm$  standard error mean. \* $P < 0.05$ , \*\* $P < 0.01$ , \*\*\* $P < 0.001$ ; one-way analysis of variance followed by the Bonferroni post-test (except J, O, P; unpaired two-tailed t-test, H; Kruskal-Wallis test followed by the Dunn test, M; left panel, as indicated and right panel; Mann-Whitney U test). \*Vehicle vs. treatment, <sup>#</sup>imatinib vs. other treatments, <sup>§</sup>dasatinib vs. CFZ. Microscopic images; n=3 (Leica DMI6000B, 30 fields/group). Blots are representative of three independent experiments (all full blots in *Online Supplementary Figure S14*). A letter P followed by a number (in N and subsequent figures) designates the patient's identity. PARP: poly (ADP-ribose) polymerase; Cyt C: cytochrome C; CC: cleaved caspase; V: vehicle; IMT: imatinib; Dasa: dasatinib; FD: freshly diagnosed, Resp: imatinib-responder, Res: imatinib-resistant.

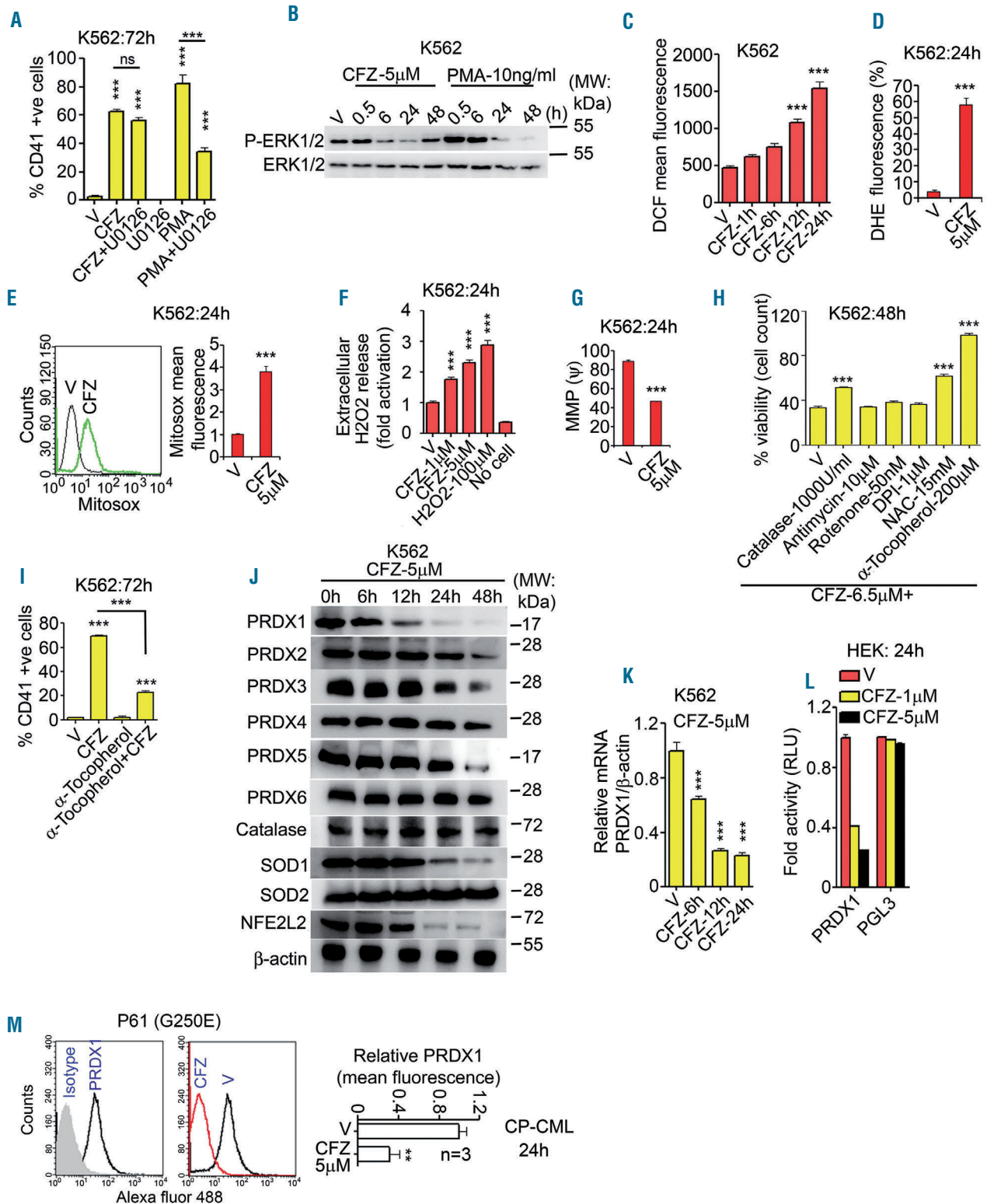


**Figure 2. Clofazimine downregulates PRDX1 expression, which leads to reactive oxygen species-dependent differentiation and apoptosis.** (A) Phorbol myristate acetate (10 ng/mL) but not clofazimine (CFZ) (2.5 μM)-induced CD41 expression in K562 cells is blocked by U0126 (10 μM; 30 min pre-treatment). Representative histograms are shown in *Online Supplementary Figure S5A*. (B) CFZ does not induce ERK phosphorylation. (C-F) CFZ induces the production of cellular reactive oxygen species (ROS). Total ROS (C); representative histograms in *Online Supplementary Figure S5B*), total superoxide (D), mitochondrial superoxide (E), and H<sub>2</sub>O<sub>2</sub> (F). (G) CFZ induces mitochondrial membrane depolarization (dot plot in *Online Supplementary Figure S5C*). (H) α-tocopherol completely blocks CFZ-induced loss of K562 viability. (I) α-tocopherol (200 μM) blocks CFZ (2.5 μM)-induced CD41 expression in K562 cells (representative histograms in *Online Supplementary Figure S5D*). (J) CFZ reduces peroxiredoxin 1 (PRDX1) protein level within 12 h. (K) CFZ reduces PRDX1 mRNA within 6 h in K562 cells. (L) CFZ reduces a PRDX1 (-1096+83) promoter-driven luciferase reporter activity in HEK-293 cells. (M) CFZ reduces PRDX1 protein in cells from patients with imatinib-resistant chronic phase chronic myeloid leukemia. Immunoblots are representative of three independent experiments. Graphs illustrate the mean ± standard error of mean. \*\**P*<0.01, \*\*\**P*<0.001 (A,C,F,H,I,K; one-way analysis of variance followed by the Bonferroni post-test. D,E,G,M; unpaired two-tailed Student *t*-test). V; vehicle; PMA; phorbol myristate acetate, ERK; extracellular signal-regulated kinase; MW; molecular weight; DHE; dihydroethidium; MMP; matrix metalloproteinase; DPI; diphenyleneiodonium; NAC; N-acetyl-L-cysteine; SOD; superoxide dismutase; NFE2L2; Nuclear factor erythroid 2 like 2; CP-CML; chronic phase chronic myeloid leukemia.

clofazimine altered the expression of factors that modulate cellular ROS or impart protection against them. Evaluation of peroxiredoxin thioperoxidases, which catalyze reduction of peroxynitrite, H<sub>2</sub>O<sub>2</sub> and organic hydroperoxides<sup>24,28</sup> revealed that clofazimine reduced PRDX1 expression at 12 h (Figure 2J) which coincided with clofazimine-induced ROS production (Figure 2C). Clofazimine also reduced PRDX3 (24 h), PRDX2 and PRDX5 (48 h) but not PRDX4 and PRDX6 (Figure 2J). Clofazimine suppressed cytosolic superoxide dismutase SOD1 (24 h onwards) but not mitochondrial SOD2 expression (Figure 2J). Nuclear factor erythroid 2 like 2 (NFE2L2), which regulates expression of various cytoprotective and multidrug resistant proteins,<sup>29</sup> was also downregulated by clofazimine (24 h onwards; Figure 2J). Clofazimine did not alter catalase expression (Figure 2J).

Since suppression of PRDX1 expression was the most proximal event observed (Figure 2J), we studied it in detail. Clofazimine suppressed *PRDX1* mRNA in K562 cells as early as 6 h (Figure 2K; quantitative real-time polymerase chain reaction primer sequences are listed in *Online Supplementary Table S2*) indicating that clofazimine may regulate the *PRDX1* promoter. We thus assessed clofazimine's effect in HEK-293 cells transfected with a *PRDX1* promoter-driven luciferase reporter (PRDX1-luc; -1065-+83) or an empty reporter and found that clofazimine specifically repressed the PRDX1-luc (Figure 2L), confirming that it modulates the *PRDX1* promoter. Figure 2L also indicates that factor(s) responsible for clofazimine-mediated downregulation of the *PRDX1* promoter is(are) endogenously expressed in HEK-293. Clofazimine also reduced PRDX1 protein in CML cells (Figure 2M).

### Introduction of exogenous PRDX1 ameliorates clofazimine-induced generation of cellular reactive oxygen species, differentiation and apoptosis

We next asked whether clofazimine's actions were mediated by PRDX1 and thus conducted rescue experiments with exogenous PRDX1. PRDX1 overexpression in K562 cells abrogated clofazimine-induced ROS production (Figure 3A), caspase cleavage and BAX expression (Figure 3B). Clofazimine-induced K562 apoptosis and differentiation were also blocked in PRDX1-transfected cells (Figure 3C, D and *Online Supplementary Figure S6A,B*). Consistently, clofazimine failed to induce ROS and apoptosis in PRDX1-transfected CML CD34<sup>+</sup> cells (Figure 3E-H). Given its observed protective function we investigated whether *PRDX1* expression is elevated in CML cells and found that there was a trend to increased *PRDX1* mRNA (albeit statistically insignificant) in CP-CML cells compared to healthy donor cells (Figure 3I). We also compared *PRDX1* levels in LSC versus non-LSC. Both CD34<sup>+</sup>38<sup>+</sup> and CD34<sup>+</sup>38<sup>-</sup> cells expressed significantly higher levels of *PRDX1* transcript than did CD34<sup>+</sup>38<sup>+</sup> cells (which were primarily gated monocytic cells), with the highest expression observed in the CD34<sup>+</sup>38<sup>-</sup> population (Figure 3J, *Online Supplementary Figure S6C*). These results indicate that clofazimine-mediated transcriptional repression of *PRDX1* expression plays a key role in imparting clofazimine's actions.

### Clofazimine-mediated suppression of PRDX1 expression is achieved through downregulation of MYB expression

Clofazimine decreased *PRDX1* mRNA at 6 h (Figure 2K) and suppressed a *PRDX1* promoter reporter (Figure

2L), indicating that it may regulate transcription factors that modulate the *PRDX1* promoter. A literature search revealed predicted binding sites for MYB, E2F transcription factor 1 (E2F1), glucocorticoid receptor (GR), CCAAT/enhancer binding protein alpha (CEBP $\alpha$ ), cAMP response element binding protein (CREB), activating transcription factor 4 (ATF-4) and activator protein 1 (AP-1) on the *PRDX1* promoter.<sup>30</sup> In K562 cells, clofazimine treatment decreased MYB expression from 3 h and CREB from 12 h onwards but had only a modest or no effect on GR, E2F1, C-Jun, C-Fos and ATF-4 (Figure 4A, *Online Supplementary Figure S7*).

Since MYB downregulation was the most proximal event observed which preceded PRDX1 downregulation and that MYB is endogenously expressed in HEK-293 cells,<sup>31</sup> we studied it in detail. Clofazimine reduced *MYB* transcripts in K562 cells from 1 h onwards (Figure 4B). Consistently, clofazimine suppressed a canonical MYB response element-driven reporter (3X MRE), while transfection of exogenous MYB rescued it (Figure 4C). We next assessed whether MYB could regulate *PRDX1* promoter, and introduction of exogenous MYB did indeed activate PRDX1-luc (-1065-+83) (Figure 4D). Furthermore, clofazimine downregulated PRDX1-luc in vector-transfected cells, and introduction of exogenous MYB dampened it (Figure 4D). These results indicate that MYB regulated the *PRDX1* promoter probably by directly binding to it, and clofazimine suppressed PRDX1 expression by downregulating endogenous MYB expression. We thus attempted to identify the MYB-responsive element on the *PRDX1* promoter. *PRDX1* promoter deletion-mapping revealed that MYB activated the -11-+83 but not the +9-+83 construct (Figure 4E). Analysis of the -11-+9 region revealed a sequence resembling the consensus MYB binding site "PyAACG/TG"<sup>32,33</sup> in reverse and complementary orientation; "CCGTTC", at position -8--3. Mutation of this sequence in the -11-+83 promoter reporter to "CCGggC", led to complete loss of MYB-responsiveness (Figure 4F). To further confirm that this sequence is indeed the MYB-responsive region on the *PRDX1* promoter, we constructed a reporter containing three copies of the -11-+9 sequence (PRDX-MYB-RE) and co-transfected it with MYB or empty vector and found that MYB did indeed specifically activate PRDX-MYB-RE (Figure 4G). Chromatin immunoprecipitation confirmed that MYB was recruited on the *PRDX1* promoter and that clofazimine reduced its recruitment, and consequently reduced histone H3 acetylation (indicating reduced transcription) (Figure 4H). Consistently, clofazimine reduced MYB protein in CP-CML (Figure 4I-J), and *MYB* transcript in CML CD34<sup>+</sup> cells (Figure 4K).

We next assessed whether the introduction of exogenous MYB could compromise clofazimine's actions and found that MYB overexpression in K562 cells did indeed mitigate the clofazimine-mediated decrease in PRDX1 expression and increase in caspase-3 cleavage, apoptosis, differentiation and ROS (Figure 4L-O, *Online Supplementary Figure S8A,B*). *MYB* mRNA expression in both imatinib-resistant and -responsive CP-CML cells was significantly higher than in control cells (Figure 4P). These results indicate that MYB binds to the *PRDX1* promoter and regulates its expression and clofazimine-mediated cellular functions are achieved through downregulation of MYB.

### Clofazimine reduces MYB expression by rapid degradation of p65 NF $\kappa$ B protein

Clofazimine reduced *MYB* mRNA expression from 1 h in K562 cells (Figure 4B); we therefore investigated whether it regulates any factor that regulates MYB expression itself. A literature search revealed that NF $\kappa$ B transcription factors regulate MYB expression by various mechanisms.<sup>34-37</sup> Consistent with a reported NF $\kappa$ B response element (NF $\kappa$ B-RE) in the *MYB* promoter situated at -278 to -256 bp upstream of the transcriptional start site,<sup>37</sup> tumor necrosis factor- $\alpha$  treatment, or p65/RELA

transfection activated a *MYB* (-687/+204) promoter reporter<sup>38</sup> (Figure 5A). Given that clofazimine downregulated *PRDX1* promoter luc in HEK-293 cells (Figure 2L) and that p65 is endogenously expressed in HEK-293 cells,<sup>39</sup> we investigated whether clofazimine regulates p65 expression. Clofazimine reduced p65 protein in K562 cells within 15 min, without affecting other NF $\kappa$ B family members, p50, p105 and C-Rel (Figure 5B). Clofazimine did, however, fail to alter *p65* mRNA expression (Figure 5C) indicating that clofazimine-mediated p65 downregulation may happen at a post-transcriptional or -translational level.

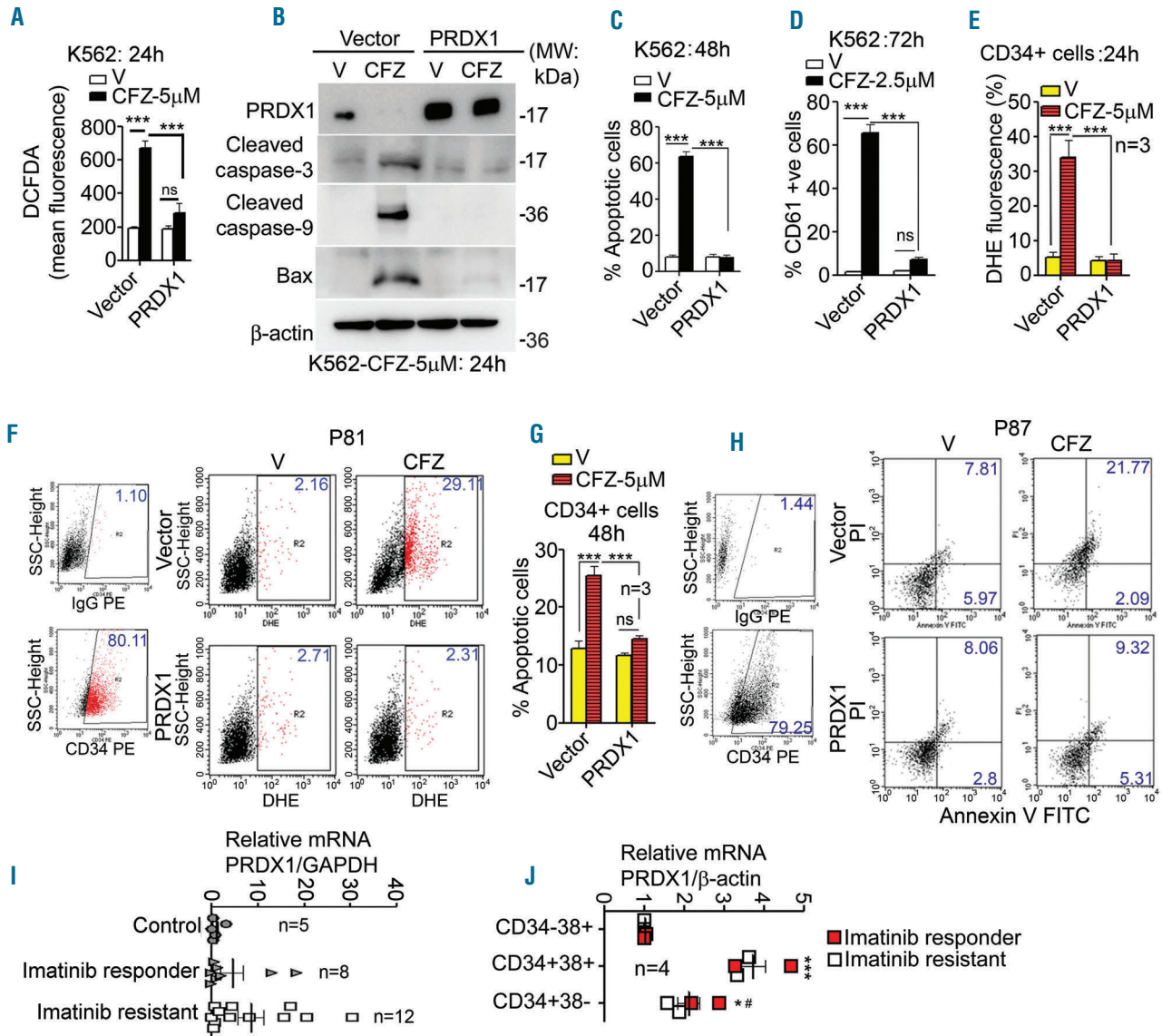


**Figure 3** Introduction of exogenous PRDX1 in cells compromises clofazimine-induced reactive oxygen species generation, apoptosis and differentiation. (A-D) Overexpression of peroxiredoxin 1 (PRDX1) in K562 cells ameliorates clofazimine (CFZ)-induced reactive oxygen species generation (A), caspase cleavage and BAX expression (B), apoptosis (C; representative dot plots in *Online Supplementary Figure S6A*), and CD61 expression (D; representative histograms in *Online Supplementary Figure S6B*). (E-H) CD34<sup>+</sup> chronic myeloid leukemia (CML) cells transfected with PRDX1 are protected from CFZ-induced ROS generation and apoptosis. (E, F) CD34<sup>+</sup> cells were isolated from chronic phase (CP)-CML cells as described above and were transfected with empty vector or a PRDX1 expression plasmid. Cells were then treated with CFZ (5  $\mu$ M; 24 h) and dihydroethidium fluorescence was measured by flow cytometry (E; graphical representation, F; representative dot plots). (G, H) CD34<sup>+</sup> cells transfected with empty vector or PRDX1 were treated with CFZ (5  $\mu$ M; 48 h) and apoptosis was assessed by annexin V staining followed by flow cytometry (G; graphical representation, H; representative dot plots). (I) *PRDX1* mRNA expression in CP-CML cells determined by quantitative real-time polymerase chain reaction (QRT-PCR). (J) *PRDX1* mRNA expression in CD34<sup>+</sup>38<sup>+</sup>, CD34<sup>+</sup>38<sup>-</sup> and CD34<sup>-</sup>38<sup>-</sup> cells by QRT-PCR. Graphs (except I & J) are mean  $\pm$  standard error of mean of three independent experiments. Immunoblots are representative of three independent experiments. \*\* $P$ <0.01, \*\*\* $P$ <0.001 (A,C,D,E,G; two-way analysis of variance followed by the Bonferroni post-test. I, J; Kruskal-Wallis test followed by the Dunn test). DCFDA: 2',7'-dichlorofluorescein diacetate; V: vehicle; SSC: side scatter; DHE: dihydroethidium; PE: phycoerythrin.



We next evaluated whether the introduction of exogenous p65 could affect clofazimine's actions and found that p65 overexpression did indeed ameliorate the clofazimine-mediated decrease in MYB and PRDX1 expression, increased caspase-3 cleavage (Figure 5H), apoptosis, differ-

entiation and ROS production in K562 cells (Figure 5I-K, *Online Supplementary Figure S9A, B*). There was a trend (albeit not statistically significant) to increased p65 mRNA in CP-CML cells compared to the level in cells from healthy donors (Figure 5L). Together, the results indicate

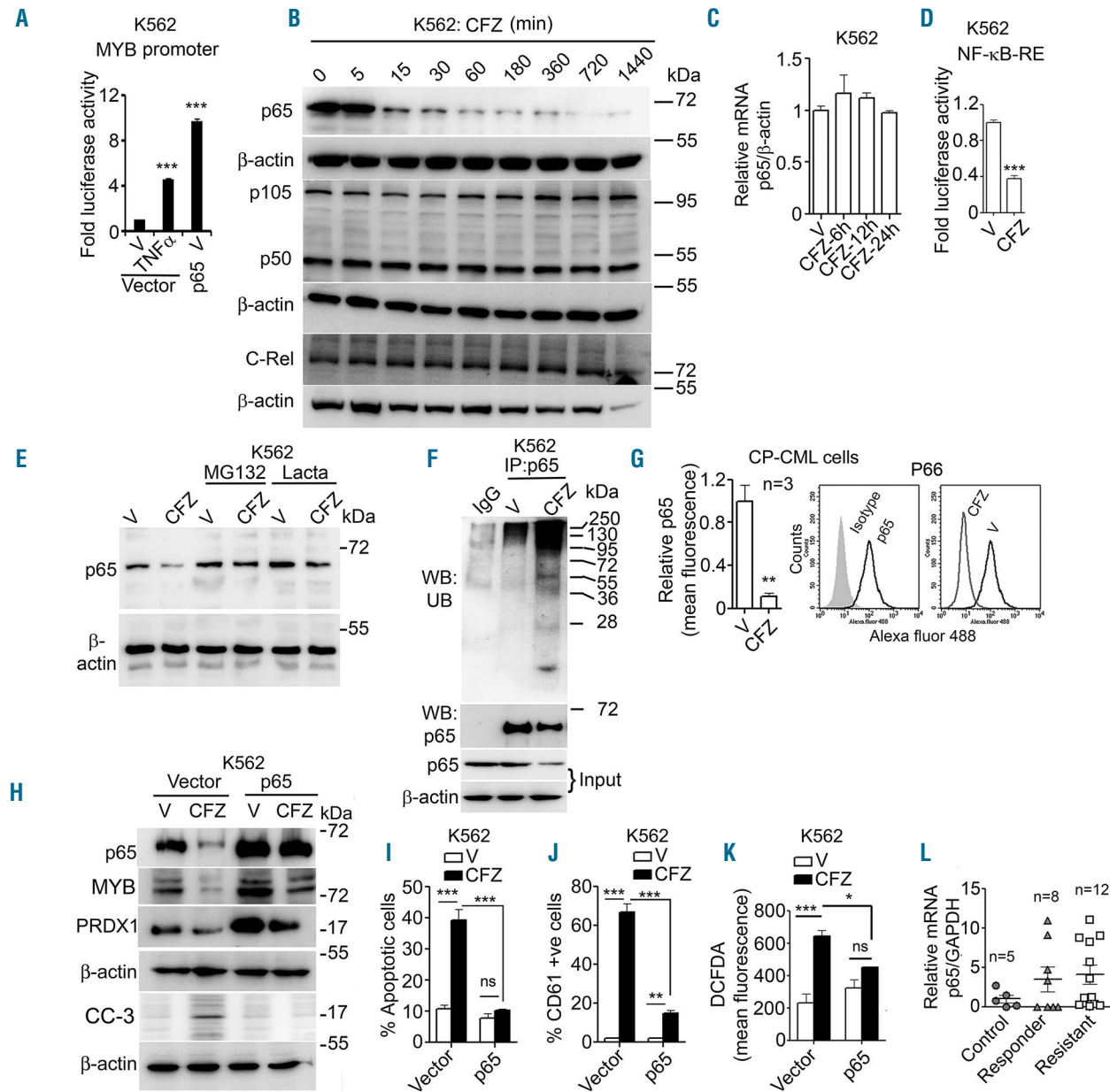


**Figure 5. Clofazimine regulates myeloblastoma oncoprotein expression via rapid proteasomal degradation of p65 NFκB.** (A) Transfected p65 or tumor necrosis factor- $\alpha$  (10 ng/mL) activates a myeloblastoma oncoprotein (MYB) promoter (-687+204)-driven luciferase reporter in K562 cells. (B, C) Clofazimine (CFZ) (5  $\mu$ M) rapidly reduces p65 protein level (B) but does not alter p65 mRNA (C) in K562 cells. (D) CFZ (5  $\mu$ M, 24 h) reduces a nuclear factor kappa B response element-driven reporter in K562 cells. (E) MG132 or lactacystin (10  $\mu$ M, 6 h pretreatment) prevents the CFZ (5  $\mu$ M, 1 h)-mediated reduction in p65 protein level in K562 cells. (F) CFZ (5  $\mu$ M, 1 h) induces ubiquitination of p65. Proteins were immunoprecipitated with a rabbit p65 antibody followed by western blotting with mouse ubiquitin or p65 antibodies. To avoid the possibility of detection of IgG heavy chain (~50 kDa), an IgG light chain-specific secondary antibody was used. (G) CFZ (5  $\mu$ M, 24 h) reduces p65 protein in imatinib-resistant chronic phase chronic myeloid leukemia (CP-CML) cells. (H-K; treatment concentration and duration same as in Figure 3A-D) p65 overexpression in K562 cells mitigates CFZ-induced downregulation of MYB and peroxiredoxin 1 and upregulation of caspase 3 cleavage (H), CFZ-mediated apoptosis (I; dot plots in *Online Supplementary Figure S9A*), CD61 expression (J; dot plots in *Online Supplementary Figure S9B*) and generation of cellular reactive oxygen species (K). (L) p65 expression in CP-CML cells. Graphs (except L) illustrate the mean  $\pm$  standard error of mean of three independent experiments. (B, E, H) are one representative of three independent experiments. (F) is one representative of two independent experiments. \* $P < 0.05$ , \*\* $P < 0.01$ , \*\*\* $P < 0.001$ . (A) One-way analysis of variance (ANOVA), (I-K) Two-way ANOVA followed by the Bonferroni post-test. (C, L); Kruskal-Wallis test followed by the Dunn test. (D, G) Unpaired two-tailed Student  $t$ -test. MYB: myeloblastoma oncoprotein; V: vehicle; NFκB: nuclear factor kappa B; TNF- $\alpha$ : tumor necrosis factor-alpha; Lacta: lactacystin; IP: immunoprecipitation; WB: western blot; UB: ubiquitin; PRDX1: peroxiredoxin 1; CC: cleaved caspase; DCFDA: 2',7'-dichlorofluorescein diacetate; GAPDH: glyceraldehyde 3-phosphate dehydrogenase.

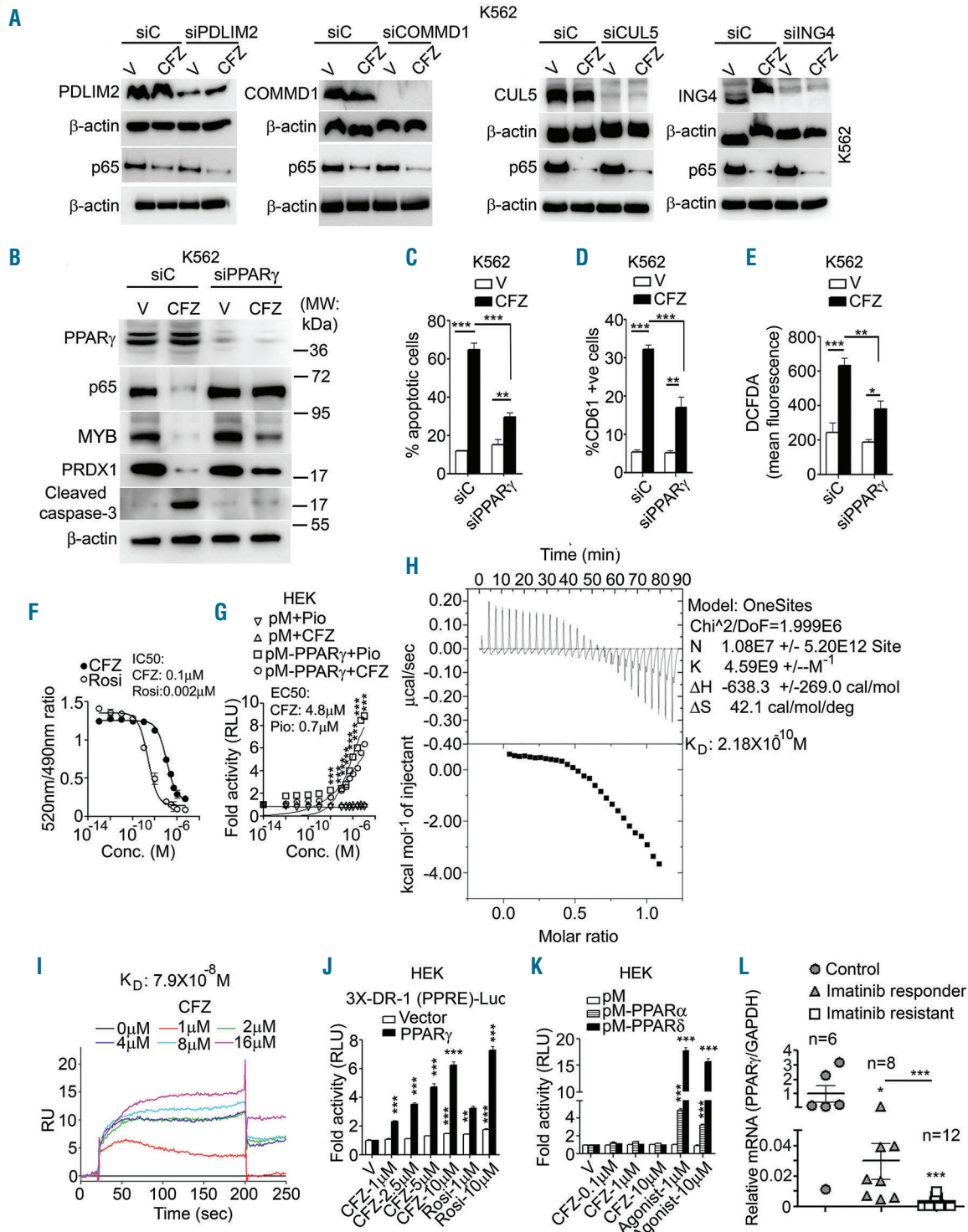


**Figure 6. Clofazimine regulates p53 level, apoptosis and differentiation via a direct interaction with PPAR $\gamma$ .** (A) Depletion of ubiquitin ligases PDLIM2, COMMD1, Cul5 and ING4 does not affect clofazimine (CFZ) (5  $\mu$ M, 24 h)-mediated decrease in p53 protein (B-E). Treatment concentration and duration same as in Figure 3A-D). Peroxisome proliferator-activated receptor (PPAR) $\gamma$  depletion in K562 cells compromises CFZ-induced downregulation of p53, myeloblastoma oncogene (MYB), and peroxiredoxin 1 (PRDX1) and upregulation of cleaved caspase-3 (B), apoptosis (C; dot plots in *Online Supplementary Figure S10A*), CD61 expression (D; histograms in *Online Supplementary Figure S10B*) and generation of reactive oxygen species (E). (F-J) CFZ physically interacts with PPAR $\gamma$  and increases its transcriptional activity. (F) The PPAR $\gamma$ -CFZ interaction as determined by a cell-free time-resolved fluorescence resonance energy transfer lanthascreen assay. (G) CFZ increases transcriptional activity of a Gal4DBD-PPAR $\gamma$ LBD fusion protein (pM-PPAR $\gamma$ ) on a GAL4 response element-containing reporter (GAL4-UAS-Luc) in transfected HEK-293 cells (H) CFZ alters thermodynamic properties of purified PPAR $\gamma$ LBD. Isothermal titration calorimetry to probe interaction of CFZ with PPAR $\gamma$ LBD (protein purification and characterization in *Online Supplementary Figure S11A-D*); CFZ (250  $\mu$ M) was titrated into PPAR $\gamma$ LBD solution (50  $\mu$ M). The titration curve shows a series of endothermic reactions followed by exothermic isotherms. (I) The interaction between PPAR $\gamma$ LBD and CFZ was evaluated using a Biacore 3000 instrument. SPR sensorgram curves showing the interactions between the indicated concentrations of CFZ and his-tagged PPAR $\gamma$ LBD captured over an anti-his antibody immobilized CM5 chip. (J) CFZ increases three-copy DR-1 PPRE luciferase activity in HEK-293 cells transfected with a PPAR $\gamma$  expression plasmid. (K) CFZ does not alter transcriptional activities of PPAR $\alpha$  or PPAR $\delta$  (agonists used; GW7647 for PPAR $\alpha$  and GW0742 for PPAR $\delta$ ; all treatments 24 h). (L) PPAR $\gamma$  mRNA expression in CP-CML cells. Graphs (except L) are mean $\pm$ SEM of three independent experiments. Blots are one representative of three independent experiments. (H-I) One representative of two independent experiments. \* $P$ <0.05, \*\* $P$ <0.01, \*\*\* $P$ <0.001 (C-E, G). Two-way analysis of variance (ANOVA), (J-K) One-way ANOVA followed by the Bonferroni post-test. L; (K) Kruskal-Wallis test followed by the Dunn test.

that clofazimine causes p65 proteasomal degradation by ubiquitinating it, which leads to sequential MYB and PRDX1 downregulation, ultimately resulting in the cellular effects imparted by clofazimine.

### Clofazimine functions through a direct interaction with PPAR $\gamma$ .

Since clofazimine induced p65 ubiquitination (Figure 5F), we next investigated whether clofazimine modulated any of the E3 ubiquitin ligases that are reported to ubiquitinate p65. PDZ and LIM domain protein 2 (PDLIM2), inhibitor of growth family member 4 (ING4), cullin 5 (CUL5), copper metabolism domain containing 1 (COMMD1; also called MURR1) and PPAR $\gamma$  ubiquitinate p65 and cause its proteasomal degradation.<sup>40,41</sup> We thus assessed whether clofazimine acted through any of these factors. While RNAi-mediated depletion of PDLIM2, ING4, CUL5 and COMMD1 failed to affect clofazimine-induced p65 degradation (Figure 6A), PPAR $\gamma$  depletion mitigated clofazimine-mediated decrease in p65, MYB and PRDX1 and increase in caspase-3 cleavage, apoptosis, differentiation and ROS (Figure 6B-E, *Online Supplementary Figure S10A, B*) indicating that clofazimine may modulate PPAR $\gamma$  activity (it is important to note here that HEK-293 cells also express endogenous PPAR $\gamma$ <sup>42,43</sup>).

We therefore evaluated whether clofazimine interacts with PPAR $\gamma$  and assessed its interaction with purified PPAR $\gamma$  protein in a cell-free, time-resolved fluorescence resonance energy transfer assay. Clofazimine successfully competed with a fluorophore-labeled PPAR $\gamma$  agonist for binding to purified PPAR $\gamma$ -LBD with an IC<sub>50</sub> of 0.1  $\mu$ M (Figure 6F). Since PPAR $\gamma$  is also a transcription factor, we assessed whether clofazimine also modulated its transcriptional activity in a heterologous system, in which the cells were transfected with pM-PPAR $\gamma$  [Gal4-DNA-binding-domain (DBD) fused to PPAR $\gamma$ -ligand-binding domain] or an empty pM vector containing Gal4-DBD, and a Gal-UAS-luc reporter containing binding sites for GAL4-DBD. Clofazimine concentration-dependently increased the GAL-UAS reporter activity in the presence of pM-PPAR $\gamma$  but not pM alone (Figure 6G). To confirm clofazimine-mediated transcriptional activation of PPAR $\gamma$  we also studied it on a direct repeat-1 (DR-1; 3-copy) PPAR response element-driven reporter (PPRE-luc) using full-length PPAR $\gamma$  and, in this case too, clofazimine increased PPRE-Luc activity in the presence of transfected PPAR $\gamma$  (a modest response was also seen in vector-transfected cells; due to endogenous PPAR $\gamma$ ) (Figure 6J). To further probe the interaction of clofazimine with PPAR $\gamma$ , we titrated clofazimine with PPAR $\gamma$ -LBD (the purification and characterization of PPAR $\gamma$ -LBD are illustrated in *Online Supplementary Figure S11A-D*) by isothermal titration calorimetry. The titration curve of clofazimine with PPAR $\gamma$ -LBD shows a series of endothermic reactions followed by exothermic isotherms (Figure 6H). Stoichiometry calculated by integrating isotherms was one: i.e., one molecule of clofazimine bound to one macromolecule of PPAR $\gamma$ -LBD. The equilibrium rate dissociation constant (K<sub>d</sub>) value was 0.2178 nM (Figure 6H). PPAR $\gamma$  also interacted with clofazimine in a surface plasmon resonance experiment (Figure 6I; the K<sub>d</sub> calculated by this method was 79 nM). Clofazimine did not alter the activities of pM-PPAR $\alpha$  or pM-PPAR $\delta$ , indicating its specificity for PPAR $\gamma$  (Figure 6K).

We next assessed whether there is any difference in

PPAR $\gamma$  mRNA expression between healthy control and CP-CML cells. A remarkably lower level of PPAR $\gamma$  transcripts was observed in the CP-CML cells than in healthy donors' cells, with the difference being more pronounced in cells from imatinib-resistant patients (Figure 6L). Together, these results demonstrate that clofazimine binds to PPAR $\gamma$  and modulates its transcriptional as well as E3 ubiquitin ligase activity and via its increased ubiquitin ligase activity PPAR $\gamma$  induces proteasomal degradation of p65 which in turn results in sequential transcriptional downregulation of MYB and PRDX1 leading to the cellular effects of clofazimine.

### Clofazimine shows superior cytotoxic activity compared to thiazolidinediones, acts in synergy with imatinib and drastically reduces quiescent CD34<sup>+</sup> cells

The PPAR $\gamma$  agonist pioglitazone synergizes with imatinib in eroding LSC by transcriptional downregulation but not dephosphorylation of STAT5.<sup>1</sup> Since clofazimine modulated PPAR $\gamma$  transcriptional activity, we determined whether clofazimine also regulated STAT5 expression. As expected, clofazimine suppressed STAT5 protein (Figure 7A) and mRNA (Figure 7C) expression without altering its phosphorylation in K562 cells (Figure 7B). Consistent with the ability of PPAR $\gamma$  agonists to suppress BCL-2 expression in CML cells<sup>44</sup> clofazimine decreased BCL-2 mRNA (Figure 7C) and protein (Figure 1D). Clofazimine did not alter CrkL or BCR-ABL1 phosphorylation (Figure 7D) indicating that it is not a BCR-ABL1 inhibitor *per se*. Furthermore, like pioglitazone,<sup>1</sup> clofazimine also reduced STAT5B and other LSC maintenance factors such as HIF-1 $\alpha$ , HIF-2 $\alpha$  and CITED2 transcripts in CD34<sup>+</sup> cells from imatinib-resistant patients (Figure 7E).

We next compared the anti-CML efficacy of clofazimine with that of other PPAR $\gamma$  agonists. In a cell viability assay, clofazimine was found to be the most potent among all the PPAR $\gamma$  ligands tested. While the IC<sub>50</sub> of clofazimine was 6.08  $\mu$ M, those of rosiglitazone, troglitazone and pioglitazone were 32.28  $\mu$ M, 50.01  $\mu$ M, and 37.39  $\mu$ M, respectively (Figure 7F).

Since pioglitazone and imatinib synergistically inhibit CML cells,<sup>1</sup> we assessed whether the same was true with clofazimine. In a K562 viability assay imatinib, dasatinib and clofazimine displayed IC<sub>50</sub> values of 0.95  $\mu$ M, 0.64  $\mu$ M and 4.13  $\mu$ M respectively. However, combining 1.56  $\mu$ M clofazimine, which is close to the average human plasma level of clofazimine (0.7 mg/L) following daily oral administration of 100 mg clofazimine,<sup>6</sup> with imatinib reduced the IC<sub>50</sub> of imatinib to 36.4 pM (Figure 7G). The combination index (CI) calculated using the Compusyn program revealed CI values <1 (*Online Supplementary Table S3*), indicating a synergistic effect. Compared to clofazimine, pioglitazone (48 h) showed a rather modest effect, which although synergistic (*Online Supplementary Table S4*), only reduced the IC<sub>50</sub> of imatinib from 0.399  $\mu$ M (alone) to 0.052  $\mu$ M (with 5  $\mu$ M pioglitazone) or 0.032  $\mu$ M (with 10  $\mu$ M pioglitazone) (Figure 7H). Clofazimine also displayed synergism with dasatinib, where the IC<sub>50</sub> of dasatinib of 0.64  $\mu$ M (alone) was reduced to 0.0124  $\mu$ M in the presence of clofazimine (Figure 7G) and the calculated CI was <1 (*Online Supplementary Table S5*). We next assessed whether the combination of imatinib and clofazimine, like pioglitazone,<sup>1</sup> also eroded LSC. First, we performed a colony-forming assay in which clofazimine alone drastically reduced colony number compared to vehicle or imatinib,

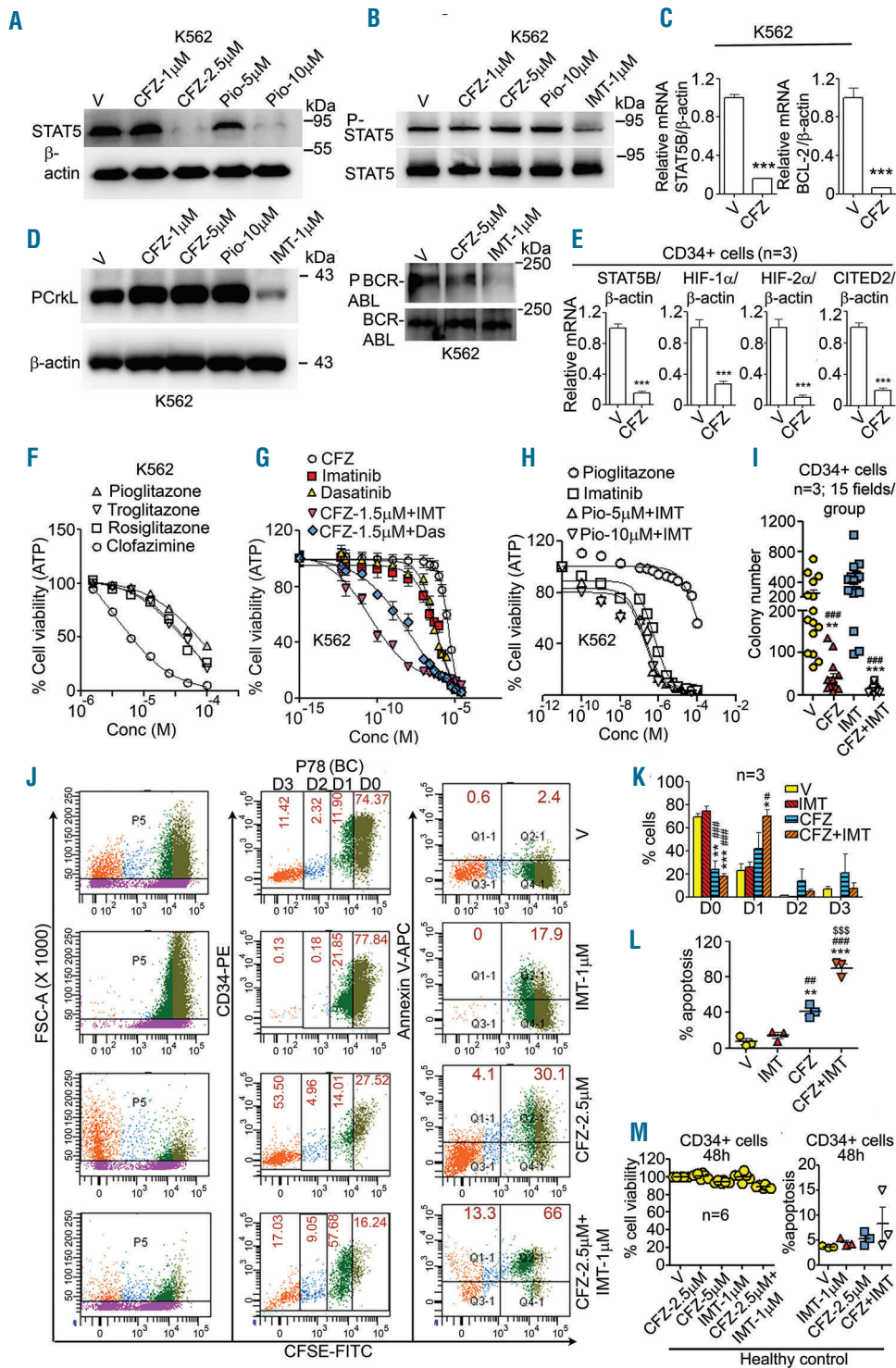


**Figure 7. Clofazimine modulates PPAR $\gamma$  target gene expression and shows synergy with imatinib.** (A) Clofazimine (CFZ) and pioglitazone (Pio) reduce signal transducer and activator of transcription 5 (STAT5) protein level in K562 cells (96 h). (B) Imatinib (IMT) but not CFZ or Pio (30 min) reduces STAT5-Y694 phosphorylation. (C) CFZ (5  $\mu$ M, 24 h) reduces STAT5B and BCL-2 transcripts in K562 cells. (D) IMT, but not CFZ or Pio (30 min), reduces Crkl-Y207 and BCR-ABL1 (ABL1-Y245) phosphorylation. (E) CFZ (5  $\mu$ M, 24 h) reduces STAT5B, hypoxia-inducible factor (HIF)-1 $\alpha$ , HIF-2 $\alpha$  and CITED2 transcripts in CD34 $^{+}$  cells isolated from IMT-resistant chronic phase chronic myeloid leukemia (CP-CML) cells. (F) CFZ (72 h) shows superior cytotoxicity to thiazolidinediones in K562 cells. (G, H) CFZ (48 h) shows superior cytotoxic synergy with IMT in K562 cells (G) than Pio (H). (I) CFZ alone or in combination with IMT reduces colony-forming cells in soft agar assay (images in *Online Supplementary Figure S2C, I*; same set of data as Figure 1H, with the addition of the CFZ+IMT group). (J-L) CFZ alone or in combination with IMT erodes the quiescent CD34 $^{+}$  population and induces apoptosis in these cells. The CD34 $^{+}$  population from IMT-resistant CP-CML cells (n=3) were labeled with 2  $\mu$ M carboxyfluorescein succinimidyl ester (CFSE) and treated as indicated (96 h). Cells were gated on the basis of CFSE intensity. The distribution (%) of CFSE/CD34 $^{+}$  cells in each cell division is shown by different colored dots (D0-D3 represent the cell division number). Apoptosis in these cells was determined by annexin V staining. (J) Representative dot plots corresponding to patient 78 (P78) who was in blast crisis. (K) Cell numbers (%) on D0-D3 from three patients (dot plots corresponding to other patients are presented in *Online Supplementary Figure S12*). (L) Percentage mean apoptosis from three patients whose data are plotted (see also *Online Supplementary Figure S12*). (M, N) CFZ alone or in combination with IMT does not alter viability (M) of CD34 $^{+}$  cells from healthy controls or induce apoptosis in these cells (N; dot plots in *Online Supplementary Figure S2D*). (M, N) Same set of data as in Figure 1K, with the addition of the CFZ+IMT group. Immunoblots are one representative of three independent experiments. Graphs are mean  $\pm$  standard error of mean of three independent experiments. \* $P$ <0.05, \*\* $P$ <0.01, \*\*\* $P$ <0.001, \*\*\*\* $P$ <0.0001. \* $V$  vs. treatment, \*IMT vs. CFZ, \*CFZ vs. IMT+CFZ. (C, E); Mann-Whitney U test. (I) Kruskal-Wallis test followed by the Dunn test. (K, L, N) One-way analysis of variance followed by the Bonferroni post test.

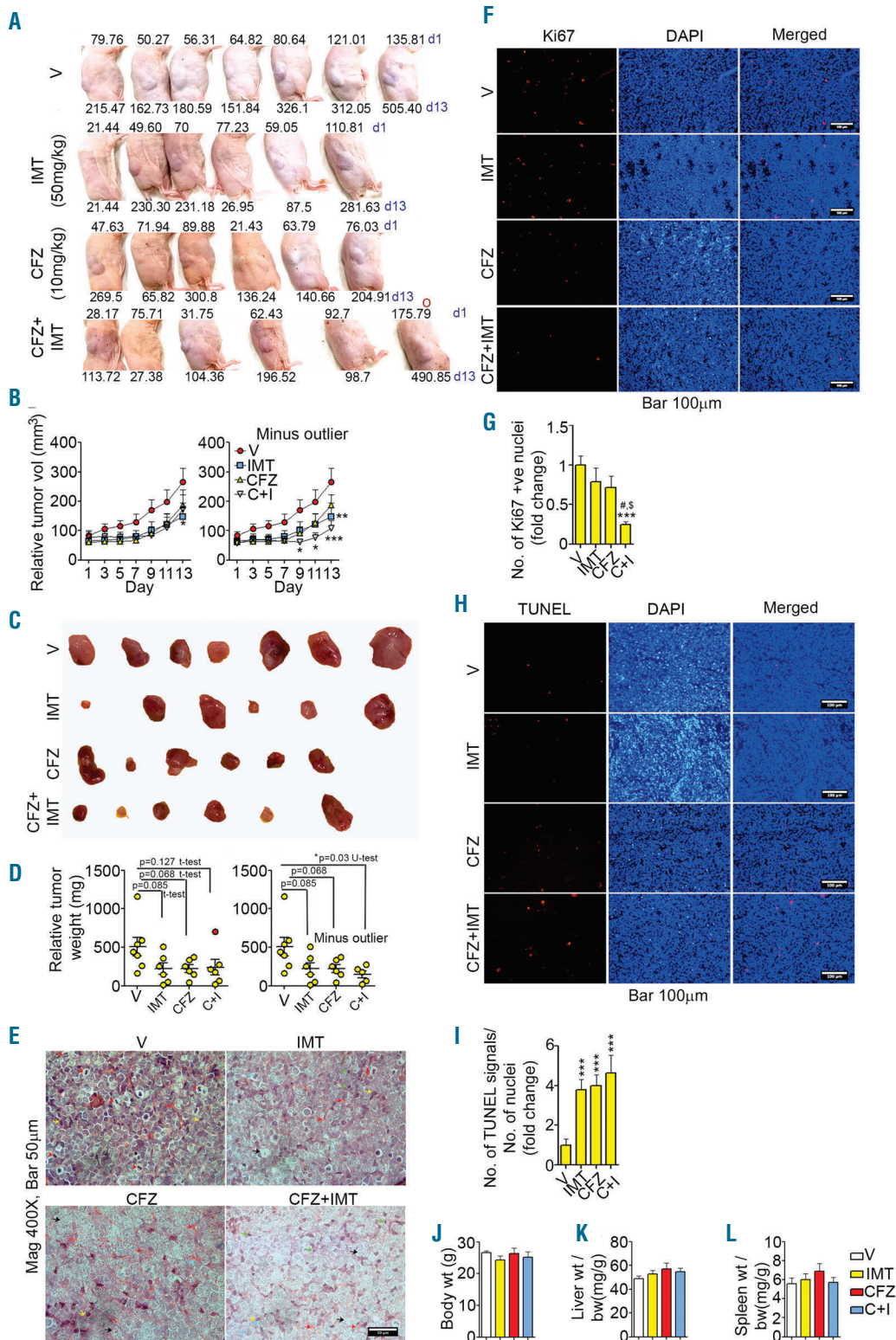


**Figure 8. Effects of clofazimine and clofazimine + imatinib on K562 xenografts.** (A) Photographs of mice with tumor, tumor volumes on day 1 (d1) and day 13 (d13) are given. The red 'O' represents an outlier based on d1 tumor volume ( $>150 \text{ mm}^3$ ). (B) Relative tumor volume (day wise), left panel; all data included, right panel; minus the outlier (as shown in A). (C) Photographs of tumors. (D) Tumor weight, left panel; all data included (outlier marked in red); right panel: minus outlier. (E) Hematoxylin & eosin staining of tumor sections (red arrowhead: mitotic cells; red arrow: vasculature; yellow arrow: myeloblasts; green arrow: pyknotic nuclei; cyan arrow: karyorrhexis; black arrow: degenerating cells). (F) Ki67 staining. (G) Number of Ki67-positive nuclei. (H) Terminal deoxynucleotidyl transferase dUTP nick end labeling (TUNEL) assay. (I) Number of TUNEL signals/ number of nuclei in a field. (E-I) Eighteen fields/group (6 animals/group). (J-L) Body weight normalized liver weight (K), and body weight normalized spleen weight. (J-L) Vehicle; n=7, all treatment groups, n=6 per group. Microscopy was performed with a Leica DMI6000B microscope (Leica) and the findings were quantified with Image J software. (F, H) For counting, intensity of all images was enhanced in Microsoft office picture manager at a mid-tone setting of 80. Cropped images with uniformly increased brightness are given here for clarity; corresponding full-size images are presented in *Online Supplementary Figure S13A*. B, \*, #, \$P<0.05, \*\*P<0.01, \*\*\*P<0.001. (B) Two-way analysis of variance (ANOVA), (J-L) One-way ANOVA followed by the Bonferroni post-test, (D) As indicated. (G, I) Kruskal-Wallis test followed by the Dunn test.

and combining clofazimine with imatinib caused a further reduction (Figure 7I, *Online Supplementary Figure S2C*) (although the difference in effect of clofazimine vs. clofazimine + imatinib was not statistically insignificant, the *P* values for the differences in effect between vehicle vs. clofazimine and for vehicle vs. clofazimine + imatinib were  $P < 0.01$ – $0.001$  and  $P < 0.001$ , respectively).

We next evaluated whether clofazimine alone or in combination with imatinib could erode quiescent LSC. To that purpose, we labeled CD34<sup>+</sup> cells from imatinib-resistant patients (one patient in blast crisis) with carboxyfluorescein succinimidyl ester (CFSE) and treated them with the indicated drugs for 96 h. While imatinib failed to reduce CFSE<sup>bright</sup> (non-dividing) cells, clofazimine alone or in combination with imatinib drastically reduced their number and increased the CFSE<sup>dim</sup> (dividing cell) population (Figure 7J, K, *Online Supplementary Figure S12*). Evaluation of apoptosis in these cells revealed that clofazimine alone caused apoptosis in both CFSE<sup>bright</sup> and CFSE<sup>dim</sup> cells while combining clofazimine with imatinib caused their near obliteration (Figure 7L, *Online Supplementary Figure S12*). Clofazimine + imatinib did not affect normal CD34<sup>+</sup> hematopoietic progenitors from healthy donors as clofazimine alone or in combination with imatinib caused <14% loss of viability (Figure 7M) and did not induce apoptosis in them (Figure 7N, *Online Supplementary Figure S2D*).

#### Effect of clofazimine and the combination of clofazimine and imatinib in K562 xenografts

To assess the effect of clofazimine, imatinib or their combination *in vivo*, athymic nude (nu/nu) mice harboring K562 xenografts were orally administered vehicle (0.5% methyl cellulose), imatinib (50 mg/kg/day; roughly equivalent to a human dose of 200 mg), clofazimine (10 mg/kg/day, human equivalent dose of 50 mg) or a combination of clofazimine and imatinib (10 mg/kg/day and 50 mg/kg/day, respectively) for 12 days. Analysis of tumor volume revealed a decreasing trend in all treatment groups which although not statistically significant (except for the imatinib group in which the tumor volume was statistically significantly reduced on day 13), became so after removal of an outlier (starting tumor volume >150 mm<sup>3</sup>, marked as red 'O', Figure 8A) in the clofazimine + imatinib group in which the reduction in tumor volume was statistically significant from day 9 onwards, while that in the imatinib group was statistically significant on day 13 only (Figure 8A, B). Analysis of tumor weight (tumor images in Figure 8C) showed a similar pattern, with a decreasing trend in all treatment groups. However, upon removal of the outlier (marked red in Figure 8D, left panel and corresponding to the tumor shown in Figure 8A) a statistically significant reduction was present only in the clofazimine + imatinib group (Figure 8D). Histological analysis of the tumors revealed well-defined vasculature and a substantial number of mitotic cells in the group treated with vehicle, which were reduced in treatment groups, especially in the clofazimine + imatinib group (Figure 8E). Furthermore, karyopyknosis, karyorrhexis and degenerating cells were visible in treatment groups, especially in the clofazimine + imatinib group (Figure 8E). Staining of tumor sections for the cellular proliferation marker Ki67 revealed a significant reduction in the clofazimine + imatinib group, compared to the groups treated with vehicle or the individual drugs (Figure 8F, G). Determination of

apoptotic cells by TUNEL staining revealed a significant enhancement of signals in all treatment groups (Figure 8H, I). None of the animals in any of the treatment groups showed changes in body, liver or spleen weight (Figure 8J–L). Together, these results indicate that combining clofazimine and imatinib causes a more robust anti-tumor activity than any of the drugs alone.

## Discussion

Here, we identified clofazimine as an anti-CML agent that was particularly effective in cells from imatinib-resistant patients and robustly downregulated LSC including quiescent LSC. Clofazimine exerted its effect through PPAR $\gamma$ . Recent evidence suggests that combining thiazolidinediones with tyrosine kinase inhibitors is an effective way to counter drug resistance in CML by eroding quiescent LSC that do not require BCR-ABL1 for survival.<sup>1,45</sup> Thiazolidinediones inhibit quiescent cells by transcriptional downregulation of *STAT5*, which is highly expressed in LSC, while imatinib regulates *STAT5* phosphorylation.<sup>1</sup> Combining both drugs thus causes stronger downregulation of *STAT5* targets HIF-1 $\alpha$ , HIF-2 $\alpha$  and *CITED2*, which are critical for LSC quiescence and maintenance.<sup>1</sup> Here, we show that in addition to *STAT5*, clofazimine also regulated a novel pathway by modulating PPAR $\gamma$  ubiquitin ligase activity, which resulted in ROS-dependent apoptosis via downregulation of *PRDX1*.

*PRDX1*, originally cloned from K562 cells,<sup>46</sup> was initially described as a tumor suppressor<sup>47,48</sup> but was later identified as an oncogene in various types of cancer in which its increased expression is associated with poor clinical outcome.<sup>49</sup> *PRDX1* mRNA was reported to be elevated in imatinib-resistant patients in whom no reduction in *BCR-ABL1* was co-related with higher *PRDX1* transcript.<sup>50</sup> We also observed a higher level of *PRDX1* transcripts in cells from CP-CML patients than in those from healthy donor, although the difference was not statistically significant. A significantly higher expression of *PRDX1* was also observed in both CD34<sup>+</sup>38<sup>-</sup> and CD34<sup>+</sup>38<sup>+</sup> LSC than in non-LSC, with the highest expression in CD34<sup>+</sup>38<sup>+</sup> cells. Interestingly, *PRDX1* is a secreted protein that enhances secretion of inflammatory cytokines by interacting with toll-like receptor 4.<sup>52,53</sup> Clofazimine suppression of *PRDX1* may thus explain its clinically observed anti-inflammatory functions<sup>6</sup> and the anti-LSC activities seen here. Although *PRDX1* has been well-studied in solid tumors, its function in CML is not clear and our study suggests that a detailed exploration of its role in CML progression will be important.

A plethora of reports implicate *MYB* in leukemogenesis which regulates factors such as c-Kit,<sup>54</sup> CD34,<sup>55</sup> and FLT3,<sup>56</sup> which are highly expressed in early progenitor cells and whose aberrant expression or mutations are associated with leukemia and poor clinical outcome.<sup>54–56</sup> While *MYB* overexpression induces transformation in hematopoietic cells,<sup>57,58</sup> its depletion inhibits colony growth in cells from CML patients including those in blast crisis.<sup>59,60</sup> Here we found that clofazimine suppressed *PRDX1* transcription by downregulating *MYB* expression and, for the first time, identified a specific *MYB* target sequence on the *PRDX1* promoter.

NF $\kappa$ B is one of the important downstream signaling pathways of the BCR-ABL1 oncoprotein.<sup>45,61</sup> Abnormal

NF $\kappa$ B activation has been reported in CML<sup>61</sup> and LSC.<sup>62</sup> Furthermore, p65 inhibition was shown to inhibit CML cells including those harboring the multidrug-resistant T315I BCR-ABL1 mutation.<sup>63,64</sup> Our results show that clofazimine decreased p65 protein by increasing the ubiquitin ligase activity of PPAR $\gamma$ . While thiazolidinediones increase PPAR $\gamma$  ubiquitin ligase activity at a suprapharmacological concentration of  $\geq 100$   $\mu$ M,<sup>41</sup> clofazimine was effective at a concentration of 5  $\mu$ M. Clofazimine also displayed superior cytotoxic effects than thiazolidinediones. Furthermore, combining clofazimine with imatinib reduced the IC<sub>50</sub> of imatinib by >4 logs whereas pioglitazone reduced it by 7- to 10-fold only. Combining imatinib with clofazimine in a K562 xenograft study caused greater reductions in tumor volume and weight than either drug alone, effects which were accompanied by substantially reduced proliferation and increased degenerative morphological changes in the group given combination therapy.

Pioglitazone is associated with cardiac and hepatic safety issues along with a significant risk of bladder cancer in users.<sup>3</sup> That rosiglitazone does not increase the risk of bladder cancer<sup>3</sup> indicates that this side effect is not associated with all PPAR $\gamma$  agonists. Being a phenazine derivative, clofazimine belongs to a different class of molecule. Given its superior efficacy over thiazolidinediones and

that long-term assumption of clofazimine is not associated with major adverse effects; we propose clinical evaluation of clofazimine in combination with tyrosine kinase inhibitors in CML.

### Acknowledgments

We dedicate this paper to the memory of Ranjan Kumar Bhagat. We thank Rune Toftgard, Odd Stokke Gabrielsen, Miguel Campanero, Chieko Kai, Giorgio Pochetti, David Mangelsdorf and Kimiotsu Kohno for kind gifts of plasmids. We thank Sharad Sharma and Madhav Nilkanth Mugale for help with histological analyses, and Dipak Datta and Jayanta Sarkar for useful discussions. SS acknowledges a mission-mode in-house project for cancer from CSIR, NC acknowledges funding from CSIR network project ASTHI (BSC 0201) and a grant-in-aid from the Department of Health Research-Indian Council of Medical Research (5/10/FR/5/2012-RHN/156), Government of India and AKT acknowledges funding from the CSIR network project INDEPTH. The authors acknowledge the sophisticated analytical instrument facility at CSIR-CDRI for FACS studies. HK, SoS, SC and RK were supported by fellowships from the University Grants Commission. AKS, SK, AG, SD, KL and RM were supported by fellowships from CSIR. ND acknowledges the DBT-RA Program in Biotechnology and Life Sciences for a Fellowship. CDRI communication number: 9805.

### References

- Prost S, Relouzat F, Spentchian M, et al. Erosion of the chronic myeloid leukaemia stem cell pool by PPAR $\gamma$  agonists. *Nature*. 2015;525(7569):380-383.
- Glodkowska-Mrowka E, Manda-Handzlik A, Stelmaszczyk-Emmel A, et al. PPAR $\gamma$  ligands increase antileukemic activity of second- and third-generation tyrosine kinase inhibitors in chronic myeloid leukemia cells. *Blood Cancer J*. 2016;6:e377.
- Tuccori M, Filion KB, Yin H, Yu OH, Platt RW, Azoulay L. Pioglitazone use and risk of bladder cancer: population based cohort study. *BMJ*. 2016;352(i):1541.
- Nissen SE, Wolski K. Effect of rosiglitazone on the risk of myocardial infarction and death from cardiovascular causes. *N Engl J Med*. 2007;356(24):2457-2471.
- Gopal M, Padayatchi N, Metcalfe JZ, O'Donnell MR. Systematic review of clofazimine for the treatment of drug-resistant tuberculosis. *Int J Tuberc Lung Dis*. 2013;17(8):1001-1007.
- Cholo MC, Steel HC, Fourie PB, Germishuizen WA, Anderson R. Clofazimine: current status and future prospects. *J Antimicrob Chemother*. 2012;67(2):290-298.
- Ren YR, Pan F, Parvez S, et al. Clofazimine inhibits human Kv1.3 potassium channel by perturbing calcium oscillation in T lymphocytes. *PLoS One*. 2008;3(12):e4009.
- Leanza L, Henry B, Sassi N, et al. Inhibitors of mitochondrial Kv1.3 channels induce BAX/Bak-independent death of cancer cells. *EMBO Mol Med*. 2012;4(7):577-593.
- Leanza L, Trentin L, Becker KA, et al. Clofazimine, Psora-4 and PAF-1, inhibitors of the potassium channel Kv1.3, as a new and selective therapeutic strategy in chronic lymphocytic leukemia. *Leukemia*. 2013;27(8):1782-1785.
- Smith GA, Tsui HW, Newell EW, et al. Functional up-regulation of HERG K<sup>+</sup> channels in neoplastic hematopoietic cells. *J Biol Chem*. 2002;277(21):18528-18534.
- Schaad-Lanyi Z, Dieterle W, Dubois JP, Theobald W, Vischer W. Pharmacokinetics of clofazimine in healthy volunteers. *Int J Lepr Other Mycobact Dis*. 1987;55(1):9-15.
- Yawalkar SJ, Vischer W. Lamprone (clofazimine) in leprosy. Basic information. *Lepr Rev*. 1979;50(2):135-144.
- O'Connor R, O'Sullivan JF, O'Kennedy R. The pharmacology, metabolism, and chemistry of clofazimine. *Drug Metab Rev*. 1995;27(4):591-614.
- Marcato F, Dean CA, Giacomantonio CA, Lee PW. Aldehyde dehydrogenase: its role as a cancer stem cell marker comes down to the specific isoform. *Cell Cycle*. 2011;10(9):1378-1384.
- Melemed AS, Ryder JW, Vik TA. Activation of the mitogen-activated protein kinase pathway is involved in and sufficient for megakaryocytic differentiation of CMK cells. *Blood*. 1997;90(9):3462-3470.
- Fichelson S, Freyssonier JM, Picard F, et al. Megakaryocyte growth and development factor-induced proliferation and differentiation are regulated by the mitogen-activated protein kinase pathway in primitive cord blood hematopoietic progenitors. *Blood*. 1999;94(5):1601-1613.
- Sardina JL, Lopez-Ruano G, Sanchez-Abarca LI, et al. p22phox-dependent NADPH oxidase activity is required for megakaryocytic differentiation. *Cell Death Differ*. 2010;17(12):1842-1854.
- Nurhayati RW, Ojima Y, Nomura N, Taya M. Promoted megakaryocytic differentiation of K562 cells through oxidative stress caused by near ultraviolet irradiation. *Cell Mol Biol Lett*. 2014;19(4):590-600.
- Chen S, Su Y, Wang J. ROS-mediated platelet generation: a microenvironment-dependent manner for megakaryocyte proliferation, differentiation, and maturation. *Cell Death Dis*. 2013;4:e722.
- Shibayama-Imazu T, Sonoda I, Sakairi S, et al. Production of superoxide and dissipation of mitochondrial transmembrane potential by vitamin K2 trigger apoptosis in human ovarian cancer TYK-nu cells. *Apoptosis*. 2006;11(9):1535-1543.
- Dabrosin C, Ollinger K. Protection by alpha-tocopherol but not ascorbic acid from hydrogen peroxide induced cell death in normal human breast epithelial cells in culture. *Free Radic Res*. 1998;29(3):227-234.
- Makpol S, Zainuddin A, Rahim NA, Yusof YA, Ngah WZ. Alpha-tocopherol modulates hydrogen peroxide-induced DNA damage and telomere shortening of human skin fibroblasts derived from differently aged individuals. *Planta Med*. 2010;76(9):869-875.
- da Silveira Vargas F, Soares DG, Ribeiro AP, Hebling J, De Souza Costa CA. Protective effect of alpha-tocopherol isomer from vitamin E against the H<sub>2</sub>O<sub>2</sub> induced toxicity on dental pulp cells. *Biomed Res Int*. 2014;2014:895049.
- Liou GY, Storz P. Reactive oxygen species in cancer. *Free Radic Res*. 2010;44(5):479-496.
- Trachootham D, Alexandre J, Huang P. Targeting cancer cells by ROS-mediated mechanisms: a radical therapeutic approach? *Nat Rev Drug Discov*. 2009;8(7):579-591.
- Panieri E, Santoro MM. ROS homeostasis and metabolism: a dangerous liaison in cancer cells. *Cell Death Dis*. 2016;7(6):e2253.
- Shi X, Zhang Y, Zheng J, Pan J. Reactive oxygen species in cancer stem cells. *Antioxid*

- Redox Signal. 2012;16(11):1215-1228.
28. Hofmann B, Hecht HJ, Flohe L. Peroxiredoxins. *Biol Chem.* 2002;383(3-4):347-364.
  29. Ma Q. Role of nrf2 in oxidative stress and toxicity. *Annu Rev Pharmacol Toxicol.* 2013;53:401-426.
  30. Kim JH, Bogner PN, Baek SH, et al. Up-regulation of peroxiredoxin 1 in lung cancer and its implication as a prognostic and therapeutic target. *Clin Cancer Res.* 2008;14(8):2326-2333.
  31. Tanno B, Sesti F, Cesi V, et al. Expression of Slug is regulated by c-Myb and is required for invasion and bone marrow homing of cancer cells of different origin. *J Biol Chem.* 2010;285(38):29434-29445.
  32. Wang QF, Lauring J, Schlissel MS. c-Myb binds to a sequence in the proximal region of the RAG-2 promoter and is essential for promoter activity in T-lineage cells. *Mol Cell Biol.* 2000;20(24):9203-9211.
  33. Deng QL, Ishii S, Sarai A. Binding site analysis of c-Myb: screening of potential binding sites by using the mutation matrix derived from systematic binding affinity measurements. *Nucleic Acids Res.* 1996;24(4):766-774.
  34. Suhasini M, Pilz RB. Transcriptional elongation of c-myb is regulated by NF-kappaB (p50/RelB). *Oncogene.* 1999;18(51):7360-7369.
  35. Pereira LA, Hugo HJ, Malaterre J, et al. MYB elongation is regulated by the nucleic acid binding of NFkB p50 to the intronic stem-loop region. *PLoS One.* 2015;10(4):e0122919.
  36. Toth CR, Hostutler RF, Baldwin AS, Jr, Bender TP. Members of the nuclear factor kappa B family transactivate the murine c-myb gene. *J Biol Chem.* 1995;270(13):7661-7671.
  37. Lauder A, Castellanos A, Weston K. c-Myb transcription is activated by protein kinase B (PKB) following interleukin 2 stimulation of T cells and is required for PKB-mediated protection from apoptosis. *Mol Cell Biol.* 2001;21(17):5797-5805.
  38. Campanero MR, Armstrong M, Flemington E. Distinct cellular factors regulate the c-myb promoter through its E2F element. *Mol Cell Biol.* 1999;19(12):8442-8450.
  39. Kim MY, Koh DI, Choi WI, et al. ZBTB2 increases PDK4 expression by transcriptional repression of RelA/p65. *Nucleic Acids Res.* 2015;43(3):1609-1625.
  40. Xu H, You M, Shi H, Hou Y. Ubiquitin-mediated NFkB degradation pathway. *Cell Mol Immunol.* 2015;12(6):653-655.
  41. Hou Y, Moreau F, Chadee K. PPAR $\gamma$  is an E3 ligase that induces the degradation of NFkB/p65. *Nat Commun.* 2012;3:1300.
  42. Camacho IE, Semeels L, Spittaels K, Merchiers P, Dominguez D, De Strooper B. Peroxisome-proliferator-activated receptor gamma induces a clearance mechanism for the amyloid-beta peptide. *J Neurosci.* 2004;24(48):10908-10917.
  43. Aprile M, Cataldi S, Ambrosio MR, et al. PPAR $\delta$ , a naturally occurring dominant-negative splice isoform, impairs PPAR $\gamma$  function and adipocyte differentiation. *Cell Rep.* 2018;25(6):1577-1592 e1576.
  44. Liu JJ, Huang RW, Lin DJ, et al. Expression of survivin and bax/bcl-2 in peroxisome proliferator activated receptor-gamma ligands induces apoptosis on human myeloid leukemia cells in vitro. *Ann Oncol.* 2005;16(3):455-459.
  45. Bitencourt R, Zalberg I, Louro ID. Imatinib resistance: a review of alternative inhibitors in chronic myeloid leukemia. *Rev Bras Hematol Hemoter.* 2011;33(6):470-475.
  46. Sauri H, Ashjian PH, Kim AT, Shau H. Recombinant natural killer enhancing factor augments natural killer cytotoxicity. *J Leukoc Biol.* 1996;59(6):925-931.
  47. Neumann CA, Krause DS, Carman CV, et al. Essential role for the peroxiredoxin Prdx1 in erythrocyte antioxidant defence and tumour suppression. *Nature.* 2003;424(6948):561-565.
  48. Cao J, Schulte J, Knight A, et al. Prdx1 inhibits tumorigenesis via regulating PTEN/AKT activity. *EMBO J.* 2009;28(10):1505-1517.
  49. Ding C, Fan X, Wu G. Peroxiredoxin 1 - an antioxidant enzyme in cancer. *J Cell Mol Med.* 2017;21(1):193-202.
  50. Mascarenhas C, Woldmar L, Almeida MH, Andrade RV, Cunha AF, De Souza CA. Evaluation of peroxiredoxins (PRDX1, PRDX2 and PRDX6) expression in patients with chronic myeloid leukemia (CML) treated with imatinib in first line. *Blood.* 2014;124(21):5545-5545.
  51. Nieborowska-Skorska M, Kopinski PK, Ray R, et al. Rac2-MRC-cIII-generated ROS cause genomic instability in chronic myeloid leukemia stem cells and primitive progenitors. *Blood.* 2012;119(18):4253-4263.
  52. Riddell JR, Wang XY, Minderman H, Gollnick SO. Peroxiredoxin 1 stimulates secretion of proinflammatory cytokines by binding to TLR4. *J Immunol.* 2010;184(2):1022-1030.
  53. Liu CH, Kuo SW, Hsu LM, et al. Peroxiredoxin 1 induces inflammatory cytokine response and predicts outcome of cardiogenic shock patients necessitating extracorporeal membrane oxygenation: an observational cohort study and translational approach. *J Transl Med.* 2016;14(1):114.
  54. Ratajczak MZ, Perrotti D, Melotti P, et al. Myb and ets proteins are candidate regulators of c-kit expression in human hematopoietic cells. *Blood.* 1998;91(6):1934-1946.
  55. Melotti P, Ku DH, Calabretta B. Regulation of the expression of the hematopoietic stem cell antigen CD34: role of c-myb. *J Exp Med.* 1994;179(3):1023-1028.
  56. Volpe G, Walton DS, Del Pozzo W, et al. C/EBP $\alpha$  and MYB regulate FLT3 expression in AML. *Leukemia.* 2013;27(7):1487-1496.
  57. Lutwyche JK, Keough RA, Hughes TP, Gonda TJ. Mutation screening of the c-MYB negative regulatory domain in acute and chronic myeloid leukaemia. *Br J Haematol.* 2001;114(3):632-634.
  58. Bussolari R, Candini O, Colomer D, et al. Coding sequence and intron-exon junctions of the c-myb gene are intact in the chronic phase and blast crisis stages of chronic myeloid leukemia patients. *Leuk Res.* 2007;31(2):163-167.
  59. Ratajczak MZ, Hijjya N, Catani L, et al. Acute- and chronic-phase chronic myelogenous leukemia colony-forming units are highly sensitive to the growth inhibitory effects of c-myb antisense oligodeoxynucleotides. *Blood.* 1992;79(8):1956-1961.
  60. Calabretta B, Sims RB, Valtieri M, et al. Normal and leukemic hematopoietic cells manifest differential sensitivity to inhibitory effects of c-myb antisense oligodeoxynucleotides: an in vitro study relevant to bone marrow purging. *Proc Natl Acad Sci U S A.* 1991;88(6):2351-2355.
  61. Kirchner D, Duyster J, Ottmann O, Schmid RM, Bergmann L, Munzert G. Mechanisms of BCR-ABL1-mediated NF-kappaB/Rel activation. *Exp Hematol.* 2003;31(6):504-511.
  62. Guzman ML, Neering SJ, Upchurch D, et al. Nuclear factor-kappaB is constitutively activated in primitive human acute myelogenous leukemia cells. *Blood.* 2001;98(8):2301-2307.
  63. Lounnas N, Frelin C, Gonthier N, et al. NF-kappaB inhibition triggers death of imatinib-sensitive and imatinib-resistant chronic myeloid leukemia cells including T315I BCR-ABL1 mutants. *Int J Cancer.* 2009;125(2):308-317.
  64. Lu Z, Jin Y, Chen C, Li J, Cao Q, Pan J. Pristimerin induces apoptosis in imatinib-resistant chronic myelogenous leukemia cells harboring T315I mutation by blocking NF-kappaB signaling and depleting BCR-ABL1. *Mol Cancer.* 2010;9:112.